NEW MEXICO INSTITUTE OF MINING AND TECHNOLOGY

DEPARTMENT OF GEOPHYSICS

SOCORRO, NM 87801

DETERMINATION OF LATERAL FLOW WITHIN VADOSE ZONE BY SEISMIC RAY TOMOGRAPY

By

Abdullah Karaman

Submitted in Partial Fulfillment of the Requirements for the Degree of Master of Science in Geophysics

May, 1989

ABSTRACT

The behavior of flow in vadose zone is quite important in protecting underground water resources against possible contamination. This flow is multidimensional due to natural soil stratification and anisotropy.

Predicting the lateral and/or downward pathway and travel time of seepage through unsaturated material, can be accomplished by following changes in seismic wave velocity with time. The difference between the velocity of unsaturated and partially saturated alluvium can trace water infiltration in arid or semi-arid climatic conditions. Seismic tomography, as shown in this study, can be used for velocity determination in this type of hydrologic problem.

ACKNOWLEDGMENTS

I am indebted to the Turkish Ministry of Education for providing me with a scholarship, and my parents for their encouragement and moral support.

I would like to express my deepest appreciation to my advisor, Dr. Allan R. Sanford, for introducing me to the field of seismic tomography, and to Dr. John W. Schlue for his invaluable suggestions, guidance, and fruitful discussions throughout this study.

A.K.

TABLE OF CONTENTS

1. INTRODUCTION

Predicting the pathway and travel time for fluids to move from an impoundment through unsaturated material toward the ground water can be quite difficult. This is partially attributed to difficulties in properly characterizing hydraulic properties of unsaturated material and its inherent spatial variability *(Yeh and Gelhar,1983)*. It is also due to inherent weaknesses in some predictive transport models. Laboratory and field evidences suggest that spatial heterogeneities in hydraulic properties causes infiltration to spread over large areas.

Theoretically, lateral spreading is enhanced where seepage occurs into dry materials *(Mualem,1984)*, as shown in the laboratory by *Stephens and Heerman (1988)*. *Crosby et al. (1968,1971)* concluded that pollutants from a septic tank drain field in glacial outwash deposits of the Spokane Valley, Washington, are dispersed laterally due to low soil moisture content and large capillary forces.

Stratification tends to inhibit the downward movement of seepage. *Miller and Gardner (1962)* conducted a vertical column infiltration laboratory experiment in layered soil. They showed that for a fine over coarse material, the wetting front was inhibited in movement until enough water accumulated at the interface for the surface tension to be low enough to allow movement into the underlying coarser material. The degree of inhibition was increased when the pore sizes in the lower layer were increased. Showing similar results, *Palmquist and Johnson (1962)* executed a laboratory tank experiment consisting of five layers of different diameter glass beads. Infiltrating water initially moved away from the source at nearly equal horizontal and vertical

velocities.Upon reaching a coarser layer, downward movement stopped and lateral spreading occurred.

Predicting the lateral pathway through unsaturated materials was modeled in this study by following a discrepancy with time in seismic wave velocity. This is a typical 3-D travel time inversion or seismic tomographic problem.

The seismic tomographic method is a technique for obtaining a "picture of a slice" or image of the structure (*Dines and Lytle, 1979; McMechan,1983; Worthington,1984; Bishop et al.,1985; Stewart,1985*). A classification of the tomographic method is given by *Tien When Lo et al.*, in 1988 as: 1) Ray tomography based on the ray equation and 2) Diffraction tomography. Ray tomography as well as diffraction tomography has three reconstruction algorithm : a) Series expansion, b) Direct fourier transform algorithm and c) Filtered backprojection algorithm.

The advantage of using ray tomography (Taylor expansion) is that reconstruction can be done using first arrivals only, the most easily measured seismic quantity. The velocity field obtained from seismic tomography is not highly resolved when compared with the medical tomography (or computerized tomography). The major limitations of this technique are mainly due to irregular and limited seismic coverage as well as to seismic sources which have a lower frequency than X ray sources (*Stephen, et al.,1987*)

When ray tomography is used for the geophysical applications, there are two inherent problems : 1) Rays only propagate through a limited portion of the object due to the available source - receiver configurations, and 2) high attenuation in the earth materials resulting band limited seismic

signal causes low resolution when the wavelength is incomparable to the size of the object.

Most geophysical tomographic studies published so far use the ray tomographic methods (*Dines et al.,1979; McMechan, 1983; Menke,1984; Bishop et al.,1985; Ivanson,1985,1986; Peterson et al., 1985; Chiu et al.,1986; Cottin et al., 1986; Gustavsson et al., 1986; and Ramirez, 1986*)

2. EXPERIMENT

The hydrologic field experiment has been conducted to simulate seepage of water into a stratified soil from an impoundment and to demonstrate the importance of lateral spreading of infiltration and the capability of models to predict lateral as well as vertical movement. Water was applied through a drip irrigation system at a constant flux which is approximately 100-fold less than the average saturated hydraulic conductivity of the soil profile.

The field experiment site is located west of the New Mexico Tech campus in Socorro, New Mexico, about 120 km south of Albuquerque (Figure 1) in a semi-arid environment. The area receives about 20 cm of precipitation per year and the gross annual infiltration is about 178 cm *(Parsons,1988)*. The vegetation in the area is very sparse, consisting of scattered sage and grasses. The New Mexico Tech golf course, directly to the east of the field site is irrigated for most of the year. The field site itself had never been previously irrigated. However, some natural increase in moisture content occurred at the center of the site from the spring to the fall in 1986 due to infiltration of the rain water ponded in a pit excavated in the center of the experiment site during this time period.

2.1. GEOLOGY

Figure 2 and Figure 3 (after Parsons,1988) are geologic profiles exaggerated two-fold vertically to show different layers in more detail. The profile is stratified, consisting of an upper piedmont slope facies overlying ancient Rio Grande fluvial sands. Clay lenses up to a meter thick of undetermined lateral extent are present at all depths, but mainly in the fluvial facies.

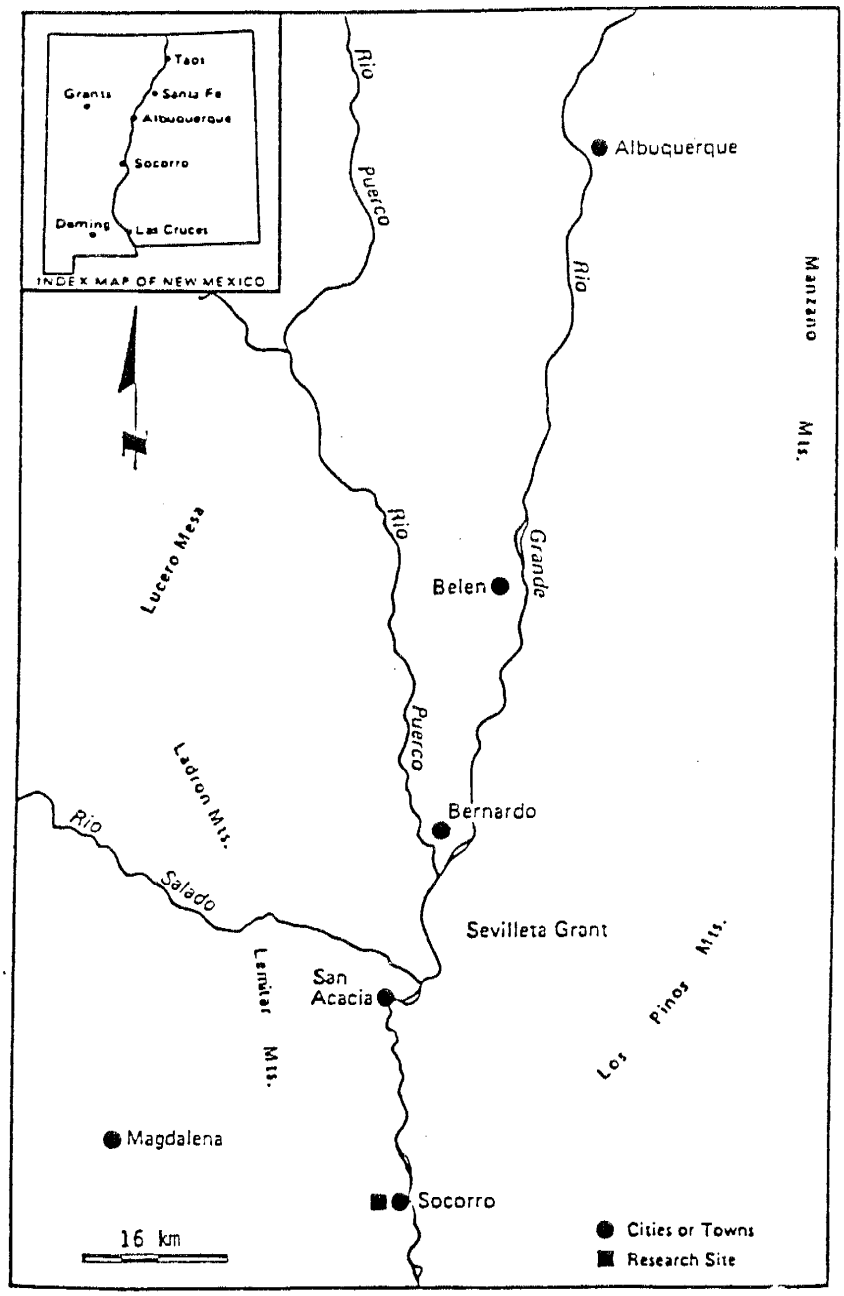

Figure 1. The index map.

There are two major cobble zones, each about one half a meter thick found beneath the entire field site. The large rocks in the cobble zones range in size from pebbles to boulders.

The piedmont slope facies is present from the surface to the position of the first major cobble zone 3 to 4 meters deep.The second cobble zone ranges in depth from 4.5 to 5.0 meters.

The piedmont slope stratification on the east-west profile (Figure 2) exhibits a slight inclination to the east. The apparent eastward inclination is presumed to reflect bedding structures from piedmont slope materials being derived from highlands directly to the west. A similar pattern does not appear to be present in the underlying fluvial sand facies, which probably were deposited in the north-south trending ancestral Rio Grande river system (Figure 3). Instead, the fluvial sands show sequences of meandering channels, consisting of well-sorted, fine sands alternating with fine to coarse sands and pebbles and overbank deposits of silts and clays. The seismic rays, in this tomographic experiment, penetrates to the depths on the order of 2 to 2.5 meters from the surface.

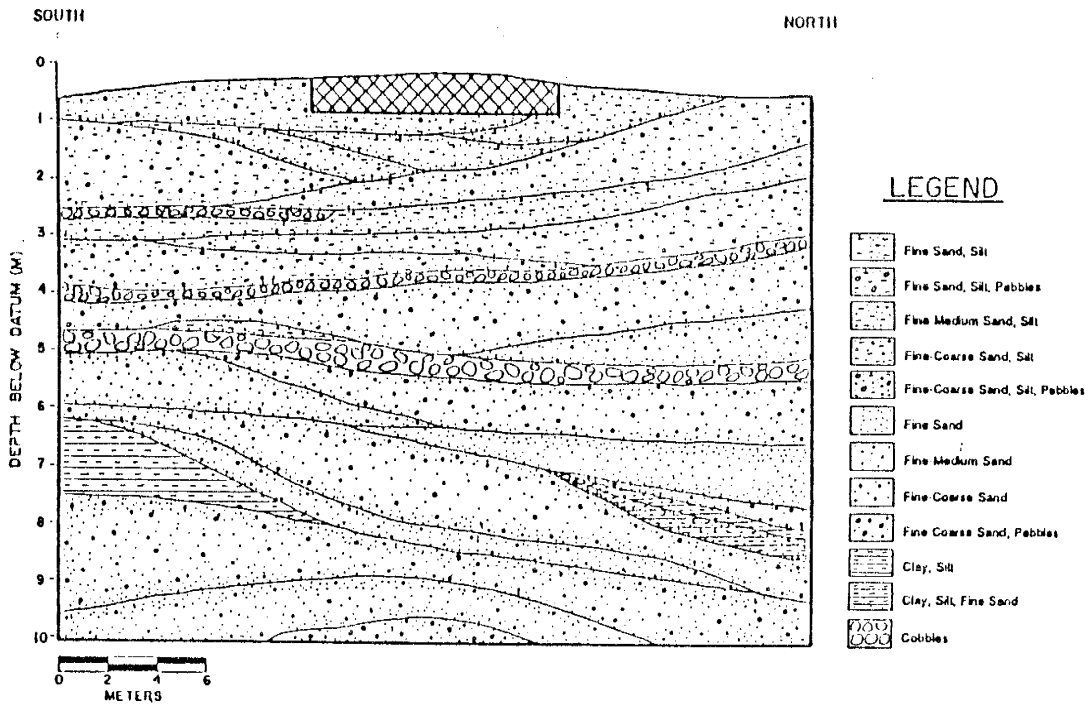

Figure 2. Geologic east-west cross-section of the experiment site (after Parsons,1988). The seismic rays in the tomographic study penetrate to depths on the order of 1-2 meters.

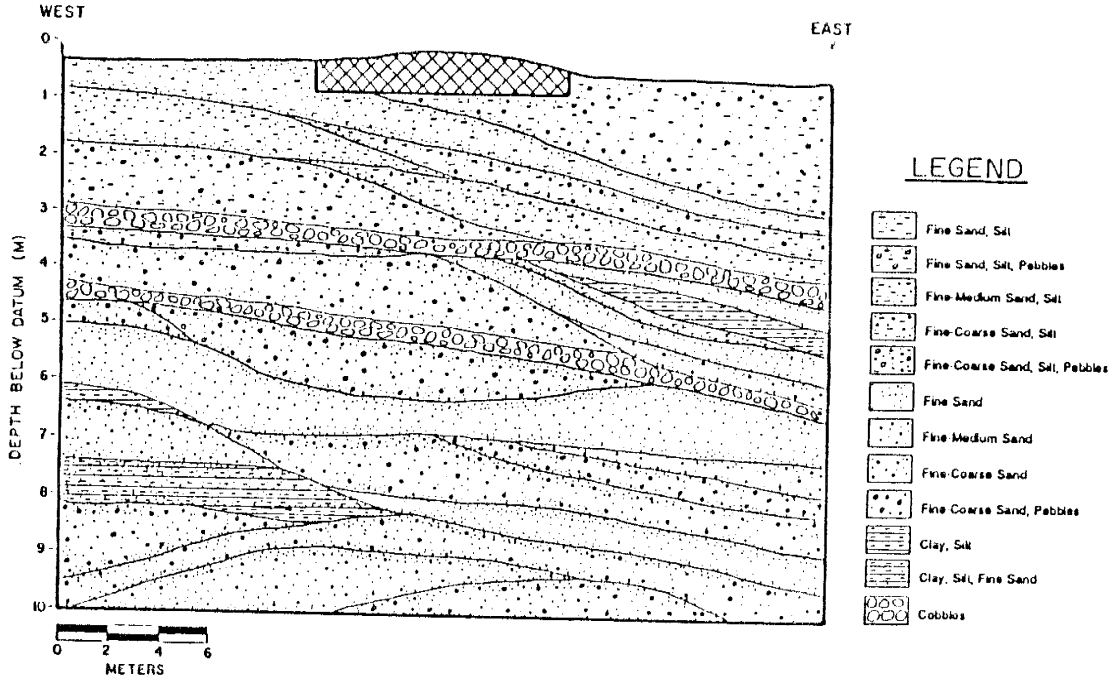

Figure 3. Geologic north-south cross-section of the experiment site (after Parsons,1988). The seismic rays in the tomographic study penetrate to depths on the order of 1-2 meters.

3. THE SEISMIC DATA

Portable 12 channel analog recorder, Geometrics ES1225, with a sledge seismic source was used for the seismic experiment. Source-receiver configurations were chosen to increase seismic coverage in the experiment site. In Figure 4, the shot and the receiver locations are based on plan view X-Y coordinate system. The solid dots are receiver locations and open triangles are the positions of the seismic sources. Each geophone line contains 12 receiver, and each geophone receives signal from the opposed five seismic sources. Drip irrigation system which is 10x10 meter in dimension remains in the area surrounded by receiver lines.

Seismic data acquisition was performed two times. The first data set containing 233 travel times was taken in October 1986, before infiltration began. One year after infiltration began, in October 1987, the same source-receiver configurations were used for the second data set containing 173 travel times. This data, unlike the first one, does not contain the records from the receiver line which is oriented to north-south on the west side of the experiment site.

The minimum distance between shots and receivers is larger than critical distance where refraction occurs.This is because critical distance does not exceed 10 meter even when extreme values of the velocity of the first an second layer are taken. Thus the seismic travel times recorded are the first arrivals of the refracted rays. The maximum depth through which the seismic ray penetrates, therefore, does not exceed 2-2.5 meters.

If the velocity throughout the experimental area was constant and remined unchanged during the infiltration, then the same arrival times at same distances would have been observed regardless of direction. How-

ever, significant velocity variations in space and generally decreasing velocity with time were observed when plotting the travel times versus their corresponding distances (Figure 5).

The shot and the receiver locations together with the ray paths are given in Figure 6. The raypath distances between shot and receiver ranged from ~ 15 meters to ~ 35 meters.

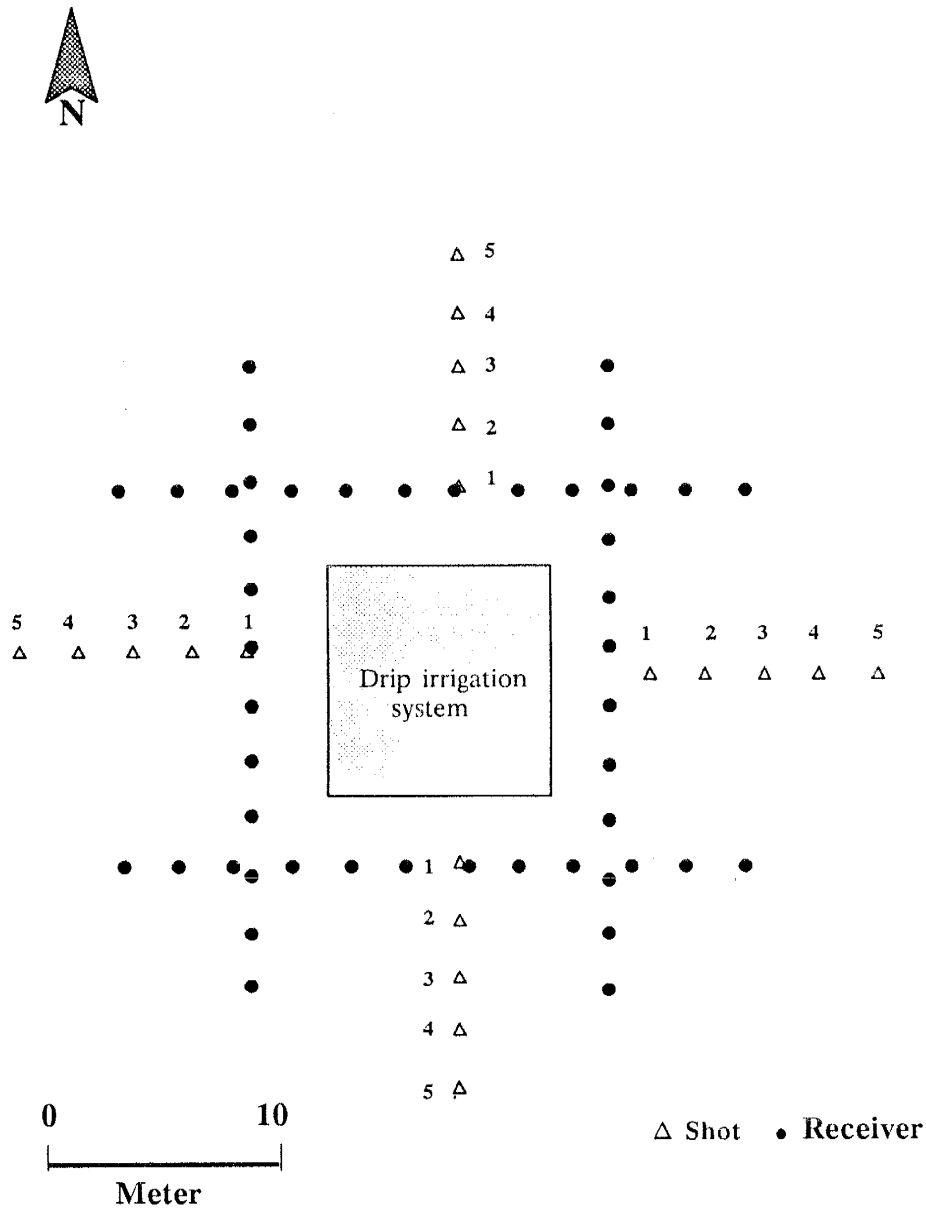

Figure 4. Source and receiver locations on X–Y plan view. Heavy line in interior outlines the wetted area. Solid dots are receiver locations and open triangles are the positions of the seismic sources.

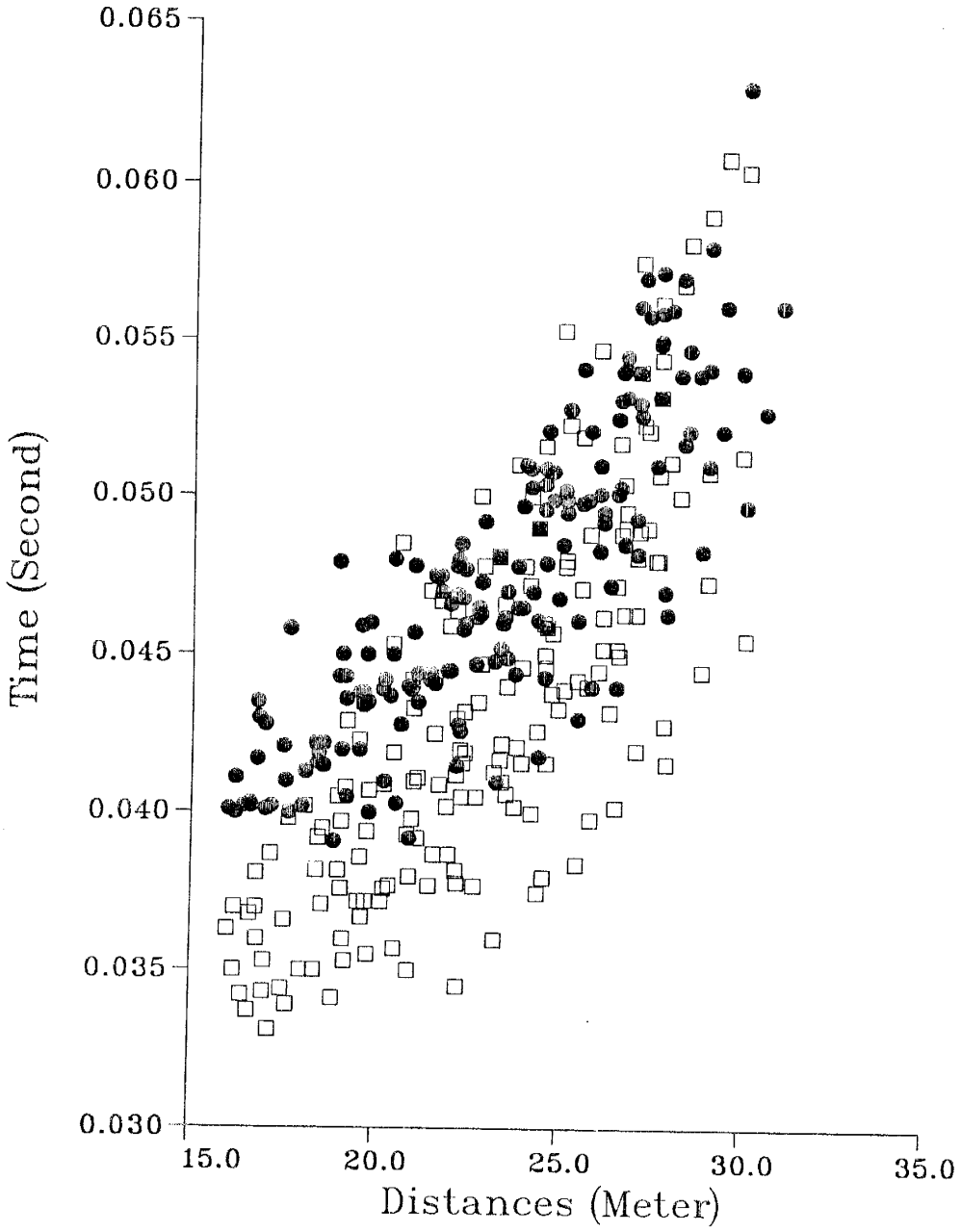

Figure 5. Travel times versus distances. The solid dots represent the arrival times after infiltration; The open squares arrival times before infiltration. The average reading error for these travel times is less then .5 millisecond.

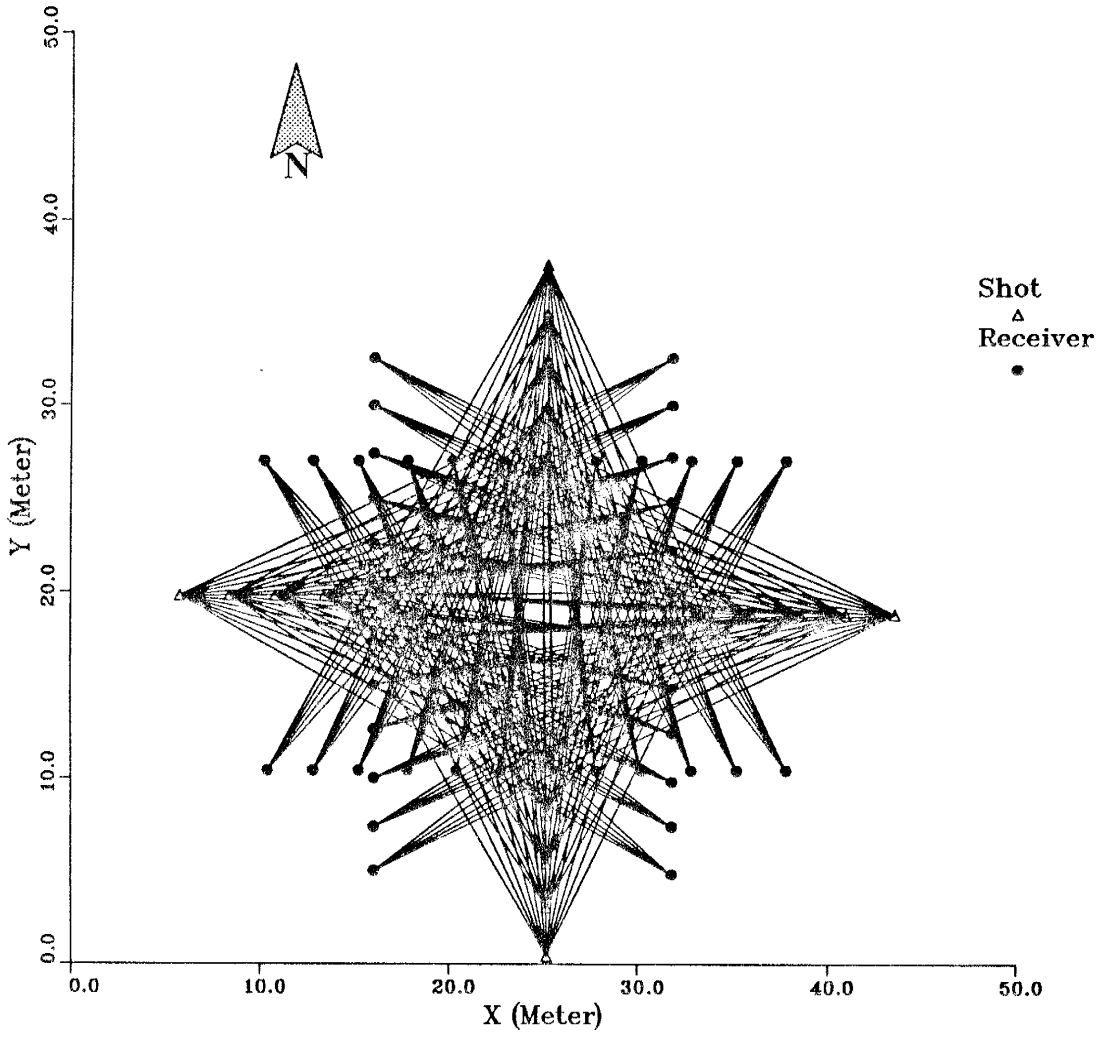

Figure 6. The ray paths in the tomographic study.

4. INVERSION ALGORITHM

Suppose that one is to calculate x_j , $J = 1, 2, \cdots M$ an unknown parameter from a set of observations Y_i , $i = 1, 2, \cdots N$. Assume the functional relation between Y_i and x_j is $Y_i(x_j)$. $Y(x)$ can be expanded to the first order Taylor expansion about x_j^o (*Chiu,et. al., 1987*) as :

$$y_i = Y_i(x_j^o) + \left.\frac{\partial y_i}{\partial x_j}\right|_{x = x^o} (x_j - x_j^o) \tag{1}$$

where

y_i : i th observation,

$Y_i(x_j^o)$: theoretical observation,

x_j^o : initial estimate of j th parameter,

x_j : updated j th parameter.

We then define :

$$\Delta x_j = x_j - x_j^o, \qquad j = 1, 2, \cdots M$$

$$\Delta Y_i = y_i - Y_i(x_j^o), \qquad i = 1, 2, \cdots N \tag{2}$$

$$A_{ij} = \frac{\partial Y_i}{\partial x_j}$$

finally :

$$\Delta Y_i = A_{i\,j}\,\Delta x_j \tag{3}$$

If we rewrite the equation 3 in matrix notation

$$\Delta \mathbf{Y} = \mathbf{A}\,\Delta \mathbf{x} \tag{4}$$

where $\Delta\mathbf{Y}$ is an $(Nx1)$ vector, $\Delta\mathbf{x}$ is an $(Mx1)$ parameter change vector, and $\mathbf{A}$ is an (NxM) matrix containing the partial derivatives.

One can use Least-Square inversion to obtain the model parameters from equation 4 by:

$$\Delta\hat{\mathbf{x}} = \begin{cases} (\mathbf{A}^{\mathbf{T}}\mathbf{A})^{-1}\mathbf{A}^{\mathbf{T}}\Delta\mathbf{Y} & , N > M \\ \mathbf{A}^{\mathbf{T}}(\mathbf{A}\,\mathbf{A}^{\mathbf{T}})^{-1}\Delta\mathbf{Y} & , N < M \\ \mathbf{A}^{-1}\Delta\mathbf{Y} & , N = M \end{cases} \tag{5}$$

where $(\mathbf{A}^{\mathbf{T}}\mathbf{A})^{-1}\mathbf{A}^{\mathbf{T}}$ and $\mathbf{A}^{\mathbf{T}}(\mathbf{A}\,\mathbf{A}^{\mathbf{T}})^{-1}$ are inverse of the non-square matrix $\mathbf{A}$, and $(\mathbf{A}^{\mathbf{T}}\mathbf{A})$ and $(\mathbf{A}\,\mathbf{A}^{\mathbf{T}})$ are always symmetric.

Since the linear equation system was derived from nonlinear case (if $Y_i\ (x_j)$ is nonlinear), first initial guess for x_j may not yield minimum residual given by ϵ, where $\epsilon_i = \Delta Y_i - A_{ij}\Delta x_j$ .The ϵ_i representing the residual error associated with each datum are due to noisy data and/or poor parameterization of the model. However, calculated residuals Δx_j can be used to compute new initial guess. This iterative process ends when model response and observed data agree within some criterion. The speed of the convergence of normal equations decreases as the relative degree of non linearity

increases. In case of too large nonlinearity, this procedure may not converge at all (*Chiu, et. al., 1986*). In case of linear relationship between model and its response , model parameters can be obtained directly from equation 5.

The problem arises when matrix $\mathbf{A}$ is singular (or ill conditioned), or does not have a full rank ($\mathbf{det}|\mathbf{A}|=0$); that is, there are certain components of solution which cannot be determined from the observations (*Wiggins, et al.,1976*). Thus $(\mathbf{A}\,\mathbf{A}^{\mathbf{T}})^{-1}$ does not exist anymore. In this case Generalized Singular Values - Singular Vectors (*Lanczos inverse, See Jackson D.,1972*) technique yields very useful tool in calculating natural inverse of matrix $\mathbf{A}$. For an arbitrary NxM system, decomposing the matrix $\mathbf{A}$ into its singular values and singular vectors yields:

$$\mathbf{A} = \mathbf{U}_{\mathbf{p}}\,\Lambda_{\mathbf{p}}\,\mathbf{V}_{\mathbf{p}}^{\mathbf{T}} \tag{6}$$

where $\mathbf{U}_{\mathbf{p}}$ and $\mathbf{V}_{\mathbf{p}}$ consist of the singular vectors corresponding to the $\mathbf{p}$ (rank of $\mathbf{A}$) positive nonzero singular values represented by diagonal matrix $\Lambda_{\mathbf{p}}$. If $\mathbf{det}|\mathbf{A}|\neq\mathbf{0}$, then both over determined and under determined case $\mathbf{p}$ = min *(M,N)*. If some of singular values are zero then $\mathbf{p}$ < min *(M,N)*. This is the case when Matrix $\mathbf{A}$ is singular ($\mathbf{det}|\mathbf{A}|=\mathbf{0}$). Since the zero singular values has been specifically excluded by taking $\mathbf{p}$, natural inverse of $\mathbf{A}$ matrix given as:

$$\mathbf{H} = \mathbf{V}_{\mathbf{p}}\,\Lambda_{\mathbf{p}}^{-1}\,\mathbf{U}_{\mathbf{p}}^{\mathbf{T}} \tag{7}$$

always exists. When $\mathbf{p} = M$ (over determined case), $\mathbf{H}$ matrix in equation 7 yields exactly Least square solution. If $\mathbf{p}=N$ (under determined), in the same way:

$$\mathbf{H} = \mathbf{V}_\mathbf{p} \Lambda_\mathbf{p}^{-1} \mathbf{U}_\mathbf{p}^\mathbf{T} \tag{8}$$

yields exactly Least square solution as well. In equation 7 and 8 $\mathbf{H}$ is called natural inverse of $\mathbf{A}$ matrix satisfying:

$$\Delta\hat{\mathbf{x}} = \mathbf{H}\,\Delta\mathbf{Y} = \mathbf{H}\,\mathbf{A}\,\Delta\mathbf{x}$$

where $\Delta\hat{\mathbf{x}}$ and $\Delta\mathbf{x}$ are estimated and true parameter vectors.

The $\mathbf{V}$ matrix, containing the orthonormal singular vectors in its columns, is a good tool to investigate model parameters resolved as a combination of each other. A unit spike located at *i* th row of *j* th vector, for example, shows that *i* th parameter is resolved without any combination of the other parameters. However, if the corresponding singular value is equal to zero, then, actually that parameter is not resolved at all. Statistically dependent data may cause broad shape in singular vectors.

The column of the $\mathbf{U}$ matrix, unlike $\mathbf{V}$ matrix, are the measure of what datum is more supportive for the corresponding singular value. Like $\mathbf{V}$ matrix, column of the $\mathbf{U}$ matrix gives no information if the corresponding singular value is equal to zero.

Matrix $\mathbf{U}$ and $\mathbf{V}$ are calculated only from matrix $\mathbf{A}$, containing the partial derivatives of the forward model respect to the concerned model

parameters. Model and geometry, therefore, can be designed by investigating these matrixes without using any real data.

Variances of model parameters given by:

$$Var\ (\hat{\mathbf{x}}_\mathbf{k}) = k^{th}\ diag\ [\mathbf{H}\ \mathbf{H}^\mathbf{T}]$$

or:

$$Var\ (\hat{\mathbf{x}}_k) = \sum_{j=1}^{p} \left(\frac{\mathbf{V}_{k\,j}}{\lambda_j}\right)^2 \tag{9}$$

where λ_j and $\mathbf{V}$ represents the singular values and singular vectors respectively. Variances of the parameters in equation 9 will be finite since $\mathbf{p}$ represents positive and nonzero singular values, but unacceptable large because of smaller singular values. To obtain acceptable variances of parameters, equation 7 or equation 8 can be written for a $\mathbf{q}$ where $\mathbf{q} < \mathbf{p}$. By doing this we exclude the smaller singular values and singular vectors such that;

$$\mathbf{H} = \mathbf{V}_\mathbf{q}\, \Lambda_\mathbf{q}^{-1}\, \mathbf{U}_\mathbf{q}^\mathbf{T} \tag{10}$$

Thus, $Var\ (\hat{\mathbf{x}}_\mathbf{k})$ in equation 9, because of excluding smaller singular values, will decrease. the $\mathbf{q}$ can be decreased for a desired maximum tolerable variances such that;

$$Var\ (\hat{\mathbf{x}}_k) = \sum_{j=1}^{q} \left(\frac{\mathbf{V}_{k\,j}}{\lambda_j}\right)^2 \leq \mathbf{t}_k \tag{11}$$

where $\mathbf{t}_k$ is maximum allowable variance of $\mathbf{x}_k$. The integer $\mathbf{q}$ is called the effective number of degrees of freedom in the data, and depends on the uncertainties in the data as well as on our need for certainty in the model.

After the decomposition of the **A** matrix, a rough idea about the matrix is practically obtained by so called Condition number (*Richard L.,et. al., 1984, page 440*), given as λ_{max} / λ_{min}. The condition number measures the stability of the problem, or the relative precision with which the matrix A defines the solution x of the equation system. In other words when condition number is large, small relative errors in A can lead to large relative errors in the solution x. The process of excluding smaller singular values, therefore, is to find U and V that minimize the condition number. In real world, when one starts excluding singular values and singular vectors, condition number given by λ_{max} / λ_q is not desired larger than ~ 500 (*Sclue J.W., Personal communication*). Threshold value $\mathbf{t}_k$ given in equation 11 and condition number may be considered together. For example, if the condition number for a **q** value is 2000 but $\mathbf{t}_k$ in equation 11 is as desired, we may not decide about the maximum tolerable variance of the parameters $\hat{\mathbf{x}}_k$ properly or smaller threshold value may be chosen.

The matrix **H** in equation 10 has a special property in investigating the "Model" and "data" when written **R = HA** and **S = AH**.

The matrix **R**, which is independent of the observations, represents the uniqueness of the resolved parameters (*Menke,1984; Schlue, J.W., et al., 1986*). If the **R** matrix is full diagonal matrix (**dig|R|=1**), that shows each parameter is resolved uniquely or independently (Least square solution). For a given **q**, if the data are statistically dependent within some degree, the rows of the **R** matrix represents the combinations of parameters resolved by the same statistically dependent data. If some of parameters are not in the

same space of the observations, then corresponding row within **R** matrix will obviously be zero. The rows of the **R** matrix are termed " Model resolution kernels".

The independence of the data is important to resolve a model parameters "*uniquely*" despite singular values excluded ($\mathbf{q} < \mathbf{p}$). The **S** matrix given by $\mathbf{S} = \mathbf{AH}$ gives an idea about the importance of each datum and degree of dependency of data. If the $\mathbf{diag}|\mathbf{S}|=\mathbf{1.0}$, then each datum is completely independent and well resolved. Broad row, located at the main diagonal is due to statistically dependence on the neighboring data, that is data are poorly resolved. Rows of **S** matrix are termed Data Resolution kernels (or information density matrix). The other importance of the **S** matrix is that it is independent of observations and only depend upon the model and geometry. Data information density matrix then may be used in investigating the importance of each observation and number of observations when considered together with the **R** matrix without making any actual observations. After setting up the model and geometry, one can investigate the **S** and **R** matrix together and decide how many observations might be made, and which of these might be more important than the others. Therefore unnecessary observations can be avoided.

I stated above that one can obtain reasonable uncertainty by keeping enough number of singular values ($\lambda_{\max}$, $\lambda_{\max-1}$, .. λ_q) and singular vectors. The cost of this process is " model dependence" or "data dependence" resolution. The quantity $\mathbf{r}_k$, $k = 1, 2, .. M$ given in following equation is the measure of the data or model dependence.

$$\mathbf{r}_k = \sum_{j=1}^{M} \left(\sum_{j=1}^{q} \mathbf{V}_{k\,j}\, \mathbf{V}_{i\,j} - \delta_{k\,i} \right)^2 \qquad (12)$$

where:

$$\delta_{k\,i} = \begin{cases} 0\,, & k \neq i \\ 1\,, & k = i \end{cases}$$

and $\mathbf{q}$ is the number of singular values kept. Calculation of the k th parameter is performed completely from the data if $\mathbf{r}_k$ = 0.0, and from the initial model if $\mathbf{r}_k$ = 1.0 . In least square case ($\mathbf{q}$ = min(M,N)) $\mathbf{r}_k$ = 0.0, that is, all parameters are calculated from the data with unreasonable uncertainty (not necessarily). If some of singular values are zero (λ_{p+1}, λ_{p+2}, .. $\lambda_{\min(M,N)}$), then corresponding parameters will be completely calculated from initial model ($\mathbf{r}_k$ = 1.). When one attempt to obtain reasonable uncertainty, compromise obviously is made between initial model and data. Plotting the $\mathbf{r}_k$'s for each parameter for different number of singular values together with respective uncertainties gives "trade - off" curves that help decide on a suitable final model. *"Trade – off"* curves compare the degree of initial model dependence and the uncertainties for each new parameter at different singular values used in the solution. Therefore initial model, obviously should be reasonable, or close enough to real values of parameters.

By now, without making any observation I gave the tools to figure out what data can resolve parameters of a given model. I gave the tools also what the uncertainties and dependence on initial model will be. If the resolving power of data is poor ($\mathbf{q} << M$), then possible improvement can be carry

out by changing only the A matrix. When one consider that uncertainties of parameters, measure of the model dependence, Model resolution Kernels (**R** matrix), Data resolution Kernels (**S** matrix), matrix **V** and **U** are completely independent of observations, it is possible to make a decision about number of observations?, additional observations?, or importance of each datum?. One may consider as well not to make some of observations which are not effective on the solution.

The Scalar R or *"goodness-of-fit"* given by the following equation 13, is the measure that how well model fits data (*Schlue, J.W., et. al., 1987*)

$$R = \left[\frac{1}{N} \sum_{i=1}^{N} \left(\frac{\Delta Y_i}{\sigma_i} \right)^2 \right]^{1/2} \qquad (13)$$

where ΔY_i represents the residual between observed and estimated data, and σ_i is the uncertainty of observed data which will be mentioned at next section. If σ_i and model are properly chosen, then the residuals between observed and estimated data, ΔY_i, may be equal to its corresponding uncertainty, that is each datum may be predicted within its corresponding uncertainty; Then the R is calculated ~1.0. In case of poor parameterization, theoretical data will be estimated too far from the observed data(assuming reasonable uncertainties of observations). Therefore R will be larger than 1.0. When too complex model is chosen (assuming proper σ_i), data then will be predicted within less uncertainty than it actually has. Thus, scalar R will be less than 1.0 . Despite well chosen model for sure, if R >> 1.0, then uncertainties of data are less than they really are.The same way, if the R << 1.0, then uncertainties of data are greater than they really are. The choice of *"good enough initial model "* may be set up if scalar R, calculated from initial model is close enough to 1.0.

4.1. WEIGHTING

It is reasonable to assume that each observation contains some noise. For example, measuring the distance between two points will vary since temperature causes expansion or contraction to the measuring tape. Therefore each measurement, in real world, has some uncertainty. In geophysics, the sources of uncertainty are usually unknown. Under some assumptions, therefore, reasonable approach can be obtained. Once decided what the source of uncertainties are for observations, these then can be used in the sense that the datum with less uncertainty can be made more dominant on the solution. In the same way, the datum with larger uncertainty can be made less effective as well. Formulation of this process is given by writing the equation 2 in the form of (*Menke, 1984*);

$$\frac{\Delta Y_i}{\sigma_i} = \frac{A_{ij}}{\sigma_i} \Delta x_j \qquad (14)$$

where σ_i is the uncertainty of observations. If uncertainty of *i* th observation is small enough, or *i* th observation is well measured, the effectiveness of this observation will be increased by dividing the corresponding observation and row within A matrix by σ_i such that the row of the A matrix and *i* th observation become larger. Therefore, the effectiveness of the datum can be increased or decreased respect to its uncertainty. Writing the equation 2 in the form of 14 makes the observations dimensionless. If this weighting is ignored, unit weighting has then been implicitly assumed.

Let say now, before inverting the data, the parameters with their uncertainties are known. By a proper weighting, symbolized by τ_j, $J = 1, 2, \cdots M$, the power of the data in calculating these pa-

rameters can be decreased or increased. Original equation 3, together with weighting by τ_j and σ_i , can be written as :

$$\frac{\Delta Y_i}{\sigma_i} = \left[\frac{\tau_j}{\sigma_i} A_{ij} \right] \left[\frac{\Delta x_j}{\tau_j} \right] \tag{15}$$

where τ_j is the uncertainty of j th parameter. The uncertainty can be any priory information about the parameter. If j th parameter in equation 15 is well known (small τ_j), then corresponding column of $\mathbf{A}$ matrix will be made close to zero. Consequently, corresponding singular value will be small enough to ignore as mentioned previously. Therefore solution will be basically model dependent ($\mathbf{r}_k$ ~ 1.0) not the data. With large uncertainty, in the same way, corresponding column will contain large values and corresponding singular value will be larger. Solution then will be more data dependent ($\mathbf{r}_k$ << 1.0). While interpreting the *trade-off* curves, this concept has to be considered. If this weighting is ignored, unit weighting has then been implicitly assumed.

5. PARAMETERIZATION OF THE PROBLEM

The velocity distribution over a ray net can be modeled by dividing the layer into a number of cells in which P wave velocity is assumed to be constant. The ray path for each shot receiver combinations are assumed to be straight. Theoretical travel times of the rays then are given by summing the values of distances/velocities for those cells traversed by the rays. The problem is generally formulated in terms of slowness (or reciprocal velocity) since travel time is a linear function of slowness. To obtain a solution one needs to have a rays which have unequal distances in cells or dissimilar rays crossing through cells. Statistical independence of the observations, therefore, is necessary in obtaining uniquely resolved final velocity model. Due to the nature of the problem solved here, acceptable solution in terms of least squares does not exist.

5.1 FORMULATION

The velocity distribution over a ray net can be modeled under the assumptions of:

1. Constant P wave velocity within each cell,
2. Straight ray path,
3. Systematic error from the first layer,
4. Under the assumptions above, uncertainties (σ_i) are only due to erroneous reading from the seismogram.

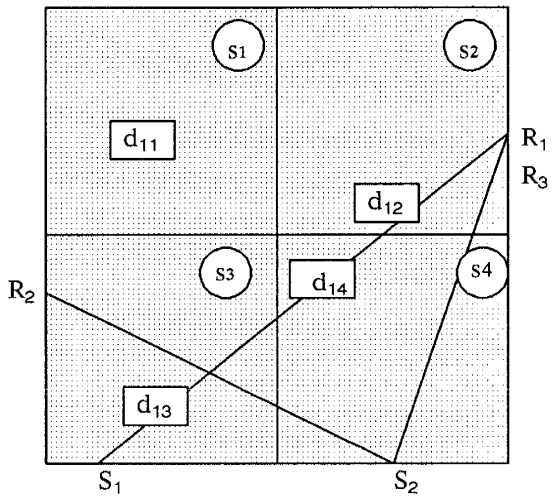

$$\begin{bmatrix} T_1 \\ T_2 \\ T_3 \end{bmatrix} = \begin{vmatrix} 0 & d_{12} & d_{13} & d_{14} \\ 0 & 0 & d_{23} & d_{24} \\ 0 & d_{32} & 0 & d_{34} \end{vmatrix} \cdot \begin{bmatrix} s_1 \\ s_2 \\ s_3 \\ s_4 \end{bmatrix}$$

Forward model corresponding to the figure

Figure 7. Symbolic shot-receiver-cell combinations.

Now from Figure 7, let s_j be the slowness (reciprocal of velocity) in cell j, T_i the measured travel time for ray i, and d_{ij} the distances that ray i travels across cell j. Let N denote the number of rays and M the number of cells. The forward model then is described by N linear equations as:

$$T_i = \sum_{j=1}^{M} d_{ij}\, s_j \qquad \begin{matrix} i = 1, 2, \ldots N \\ j = 1, 2, \ldots M \end{matrix} \qquad (16)$$

The matrix A containing the partial derivatives with respect to the slowness is given as:

$$A_{i\,j} = \frac{\partial\, T_i}{\partial\, s_j} = d_{i\,j} \tag{17}$$

and vector ΔY_i and Δx_j for travel times and slowness :

$$\begin{aligned} \Delta Y_i &= [\, t_i^{obs} - \sum_{j=1}^{M} d_{ij}\, s_j \,] \\ \Delta x_j &= (\, s_j - s_j^o \,) \end{aligned} \tag{18}$$

where s_j^o represents the initial slowness and Δx_j, $j = 1, 2, .. M$ unknown vector containing the slowness, $\mathbf{A} = d_{ij}$ and NxM matrix.

Combining the equation 17 and 18 equation 2 then is written in explicit form as;

$$[\, t_i^{obs} - \sum_{j=1}^{M} d_{ij}\, s_j \,] = d_{ij}\, (\, s_j - s_j^o \,) \tag{19}$$

is the equation solved here for slowness. Since the theoretical travel times in equation 16 are the linear function of the slowness and distances, the solution vector can be obtained from equation 19 directly.

The equation system given in 19 is neither completely overdetermined nor completely undetermined regardless of the number of observations. For example, there may be one cell through which several rays pass. This cell is clearly overdetermined. On the other hand, there may be cells that have been missed entirely. These cells are completely undetermined. There may also be cells that can not be individually resolved because every

ray that passes through one also passes through an equal distances of the other. These cells are also undetermined.

5.2. UNCERTAINTIES

In this problem, since the delay times arising from the upper layer are assumed systematic, not random, these can not be counted as source of the uncertainty. Instead, assuming that the uncertainties of the travel times are only due to the erroneous reading from the seismogram is reasonable. Different observers may place the arrival times on a seismogram at different places, for example somewhere (Figure 8) in the interval of $[\ t_p^- < t_p < t_p^+\ ]$, where t_p is average value of travel time, and t_p^- and t_p^+ are extreme readings. Then the uncertainties of t_p are given as:

$$t_p \mp |\frac{1}{2}\ [\ t_p^+ - t_p^-\ ]\ |$$

Figure 8. Symbolic arrival time and its uncertainty.

This criterion was applied to all 353 travel times to obtain the uncertainty for each travel time. If the first arrival was not clear then the extreme

values assumed were larger. For example, in the first data set the signal from forth and fifth shot of the west shot line were recorded poorly with the uncertainty of 2 millisecond. On the other hand, the rest of the arrival times in the first and the second data set have the uncertainty on the order of ~0.3 or ~0.4 millisecond in maximum.

In the section 4, the forward model was set up for the slowness. In order to convert uncertainty of velocity into uncertainty of slowness, the following general relationship was used. Let us say, f is a function of $\mathbf{x}_i$, $i = 1, 2, ..$ *i.e.*, $f = f(\mathbf{x}_i)$. If $\Delta\mathbf{x}_i$ is the uncertainty of $\mathbf{x}_i$, uncertainty of f then is given by;

$$\Delta f = \sum_{i=1} \frac{\partial f}{\partial \mathbf{x}_i} \Delta \mathbf{x}_i$$

Let us say now that s represents the slowness and v velocity. Then :

$$s\ (v) = 1\ /\ v \qquad , \qquad v = 1\ /\ s \quad ;$$

$$\Delta s = \frac{1}{v^2} \Delta v \qquad , \qquad \Delta v = \frac{1}{s^2} \Delta s$$

where Δv is uncertainty of velocity and Δs is uncertainty of slowness.

6. COMPUTATIONS

I gave so far the algorithm I used to solve a linear system together with the basis of the geometry. To perform all these calculations, I wrote two fortran program, one is inversion program which solves any linear system given in the form of $\mathbf{y}=\mathbf{A}\mathbf{x}$ by means of IMSL routines (Appendix B). Over determined and undetermined cases are controlled by the program. The input TOL is the value that if the singular values are less than TOL, they are assumed to be zero. The second program sets up the geometry; calculates the the distances that rays travels in cells. This program also was designed in very general form; the size and the number of the cells, location of the shot and receivers are completely user dependent.

Travel time inversions by use of the Lanczos inverse technique were performed three times. The first, inversion was performed by using all 233 travel times of the first data set. The results are given in Appendix A. In order to compare the final models better, the west receiver line with its 60 travel times then was excluded from the calculations since the second data set does not include these. Finally the second data set containing 180 travel times were inverted for the velocities. By removing the records of west receiver line, the results or final models become much easy to compare. The uncertainties for all data were nearly the same, except for the data obtained by the last two shots into the west receiver line which were assigned large uncertainties. The maximum tolerable standard deviation of velocities for the cells was set at 40 m/s, which is 10% of the average velocity.

6.1. VELOCITY DISTRIBUTION BEFORE INFILTRATION

After excluding records of west receiver line from the October 1986 data set, the model was set at *64 (8x8)* cells and 173 travel times. The ray paths and cells are illustrated in Figure 9. The position of the cells, shots and receivers are based on plan view X–Y coordinate system with the origin located at the southwest corner of the experiment site.

The corresponding A matrix which has 173 rows and 64 columns is given in Figure 10. The vertical axes represents the distances that ray i travels across call j. As shown in the figure, the A matrix is very sparse since some of the cells were missed. Thus, some of singular values are either zero or close to zero. During the decomposition of the matrix **A**, if the singular values were less than 1.0, they were assumed to be zero (Figure 11).

The initial standard deviations (τ_j) were assigned on the basis of prior velocity information which suggested low uncertainties beneath the shot points (Figure 12) and higher uncertainties at the center of the experiment site. By doing this, data dependent resolution was encouraged.

A 40 m/s maximum tolerable standard deviation was obtained when 23 singular values and associated singular vectors were retained with condition number 20. At final analysis, 18 of 64 cells were resolved *"uniquely"*, and the 5 other cells, resolved ~ 30% model dependent were assumed " resolved" (compare model resolution kernels with associated $\mathbf{r}_k$'s in Figure 13 and Figure 14). 41 cells as shown in these figures were resolved only from the initial model since the associated singular values were too small or zero.

Significant statistical dependency among the rays recorded by the receivers which were located on a same line was observed on the data resolution kernels (Figure 15). The configuration of the peaks located on the main diagonal of the information density matrix indicates a large degree of statistical dependency for the same geophone line but less for different geophone lines. On the other hand, the amplitudes at the main diagonal decrease as the uncertainties of associated travel times increase.

The standard deviations for each cells in meters per second are shown in Figure 16. The zero standard deviations are for the cells whose velocities are totally dictated by the initial model. On the other hand the cells resolved by the data (compare Figure 14) have relatively larger values of standard deviations but not larger than ~ 40 m/s.

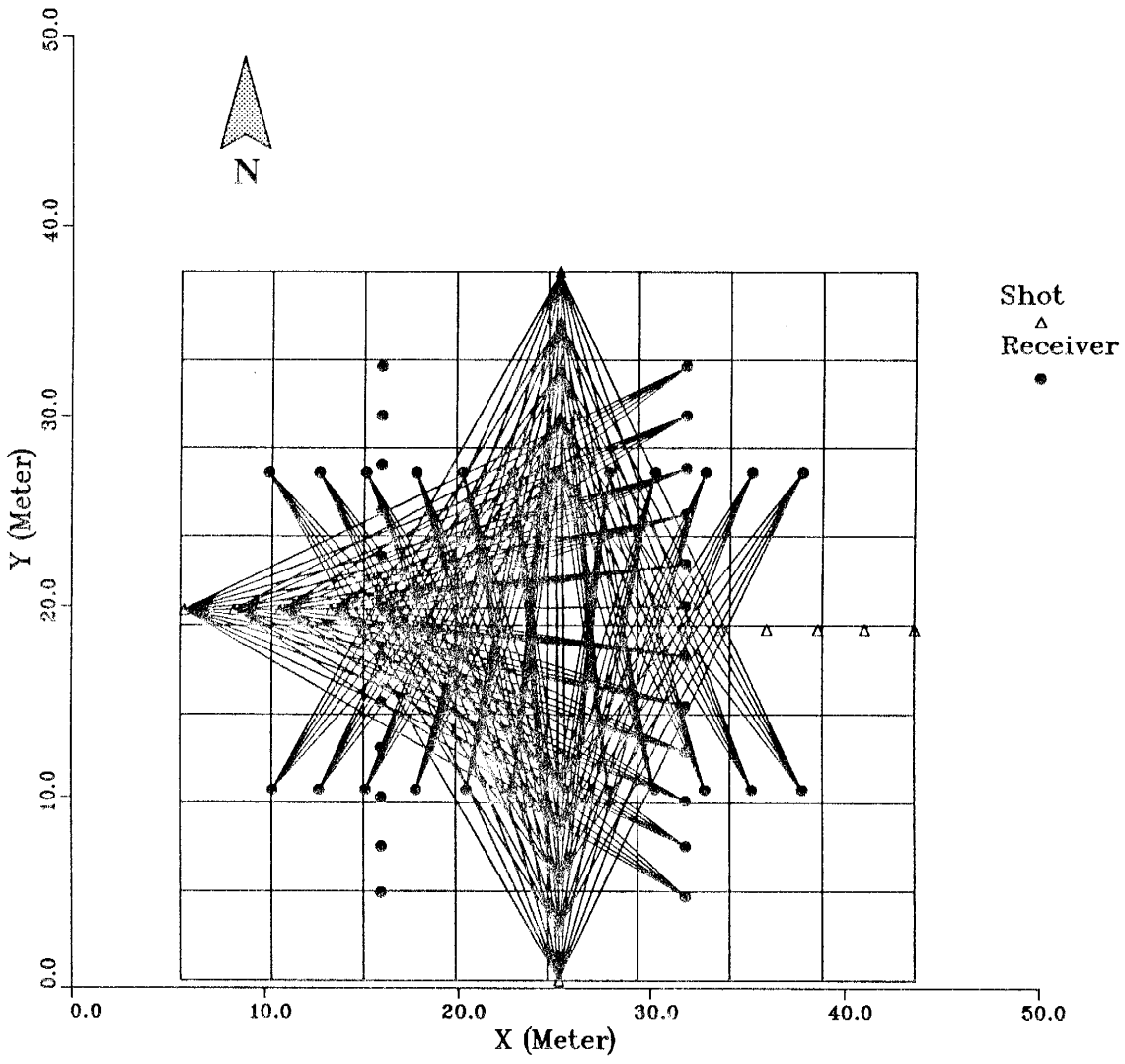

Figure 9. The model containing 173 ray and 8x8=64 cells.

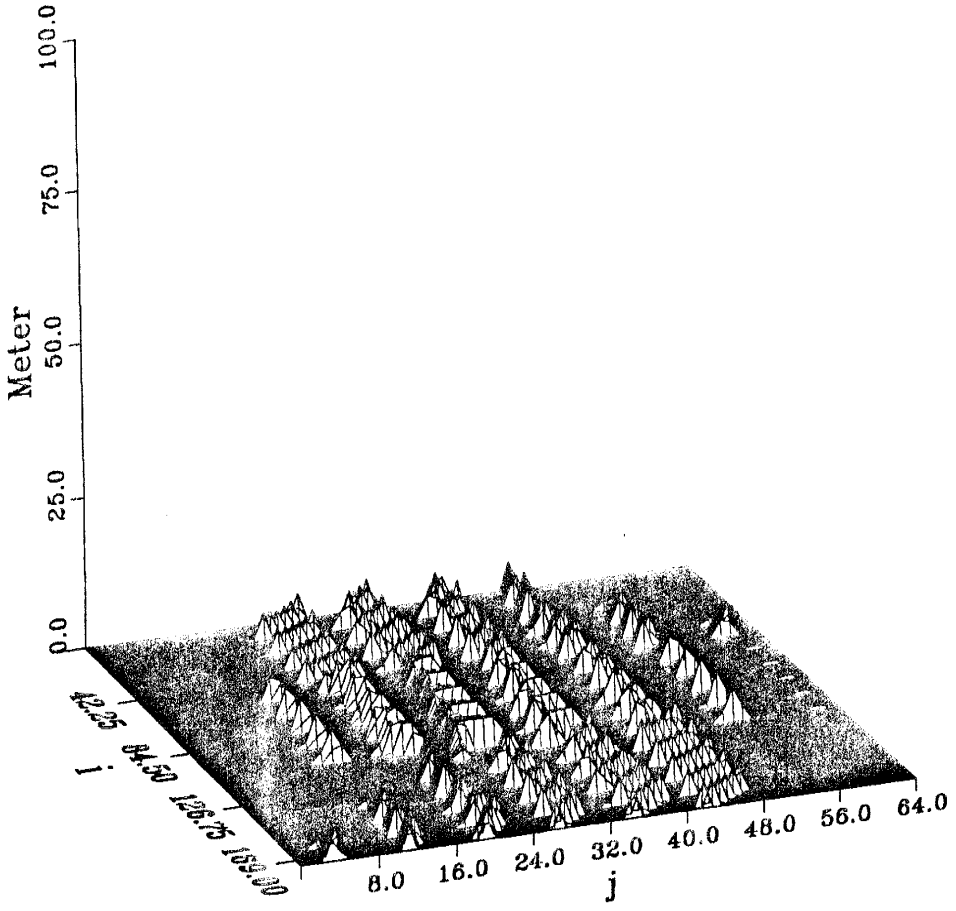

Figure 10. The A matrix. The vertical axes represents the distance in meter that ray *i* travels within cell *j*.

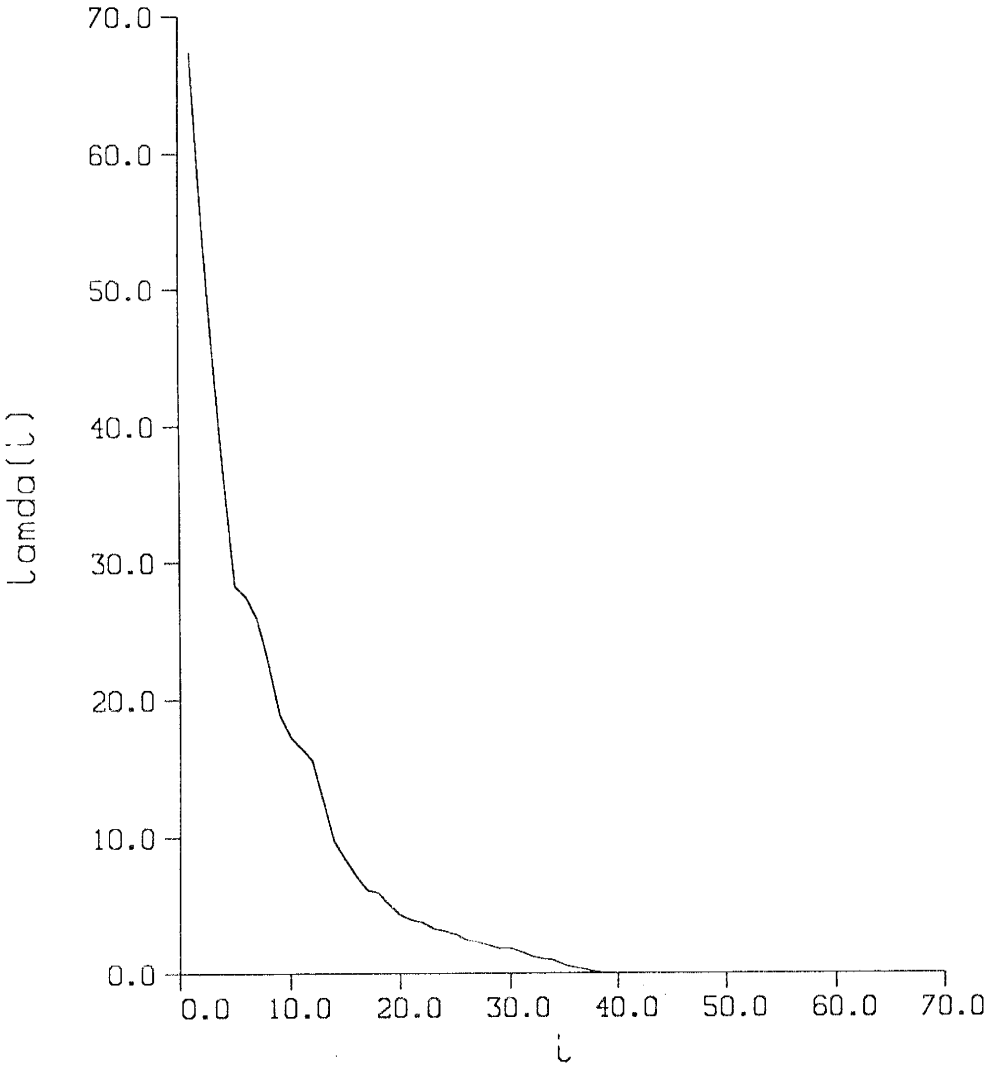

Figure 11. The singular values of the A matrix.

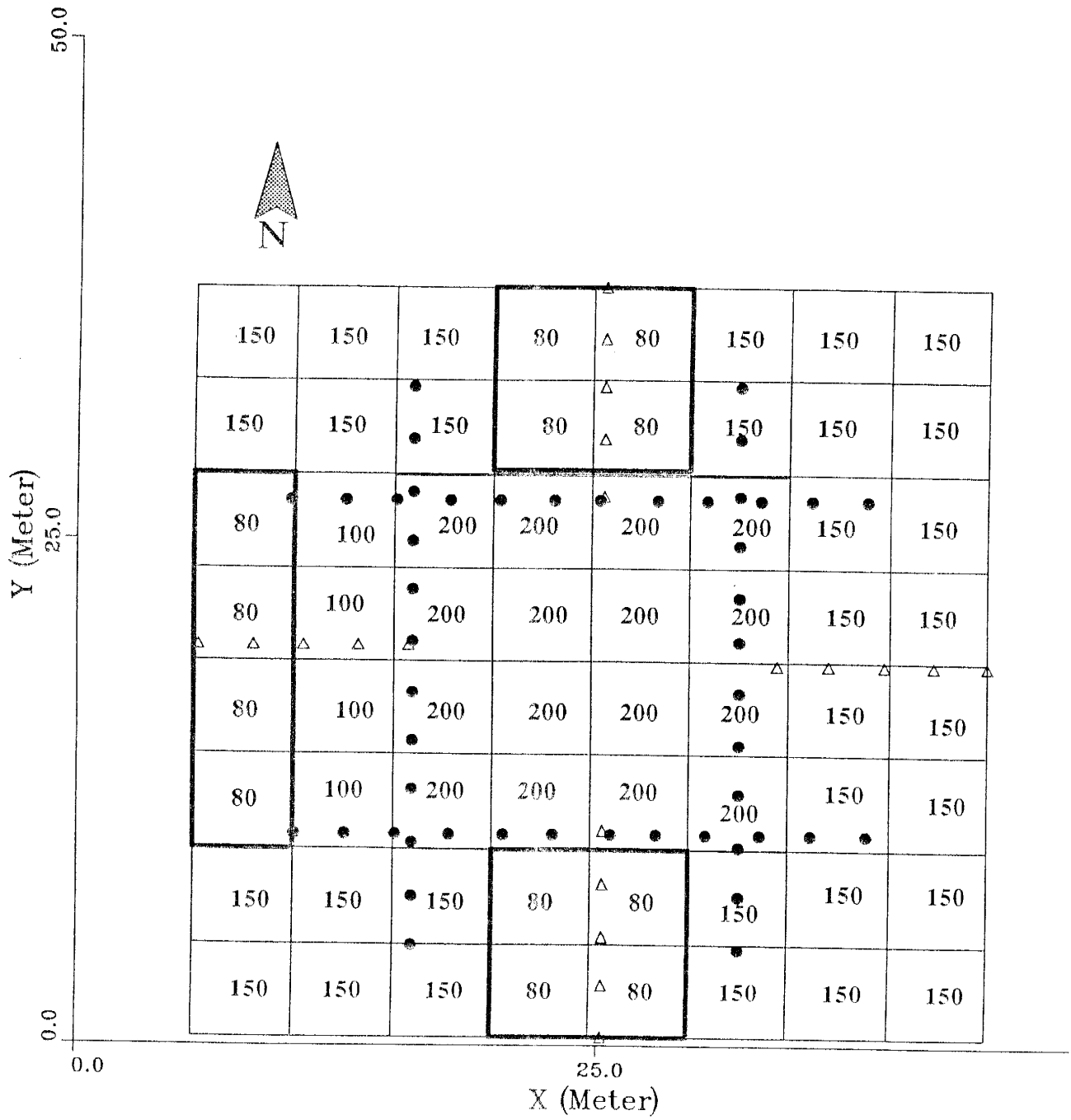

Figure 12. Initial uncertainties (τ_j 's in m/s). To obtain a data dependent resolution initial uncertainties at the experiment site were kept higher.

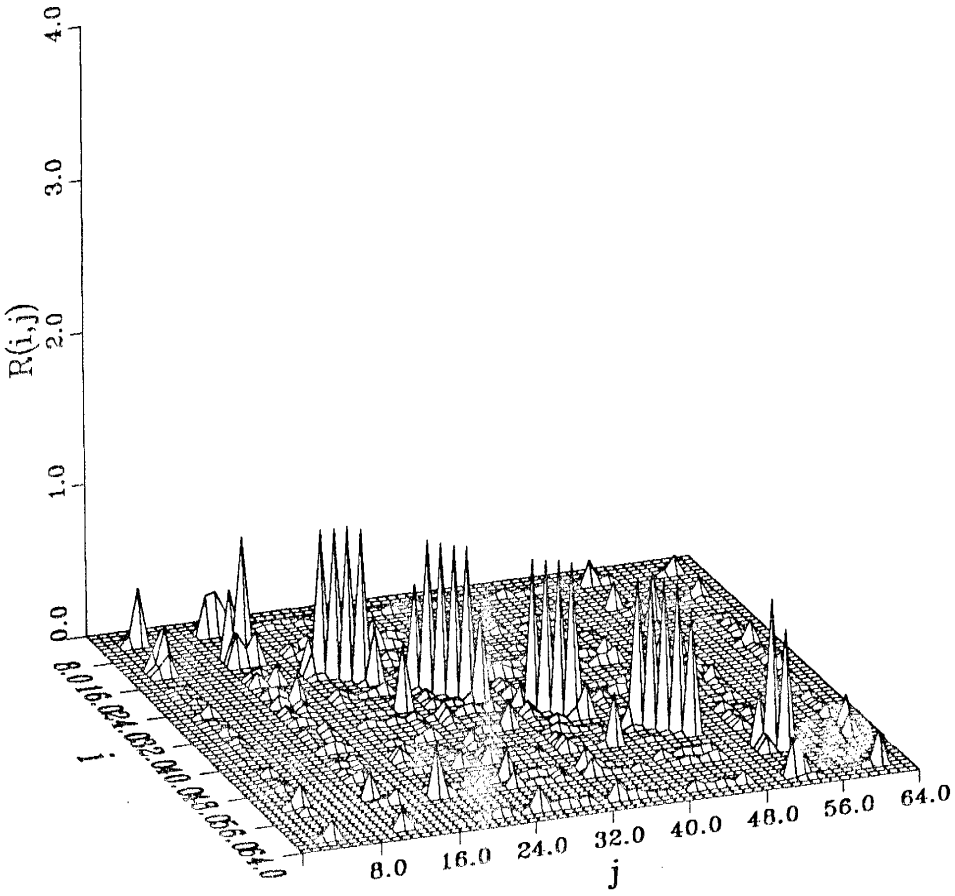

Figure 13. The absolute values of the model resolution kernels. The amplitudes of the spikes located at the diagonal are the measure of the uniqueness of the resolved parameters.

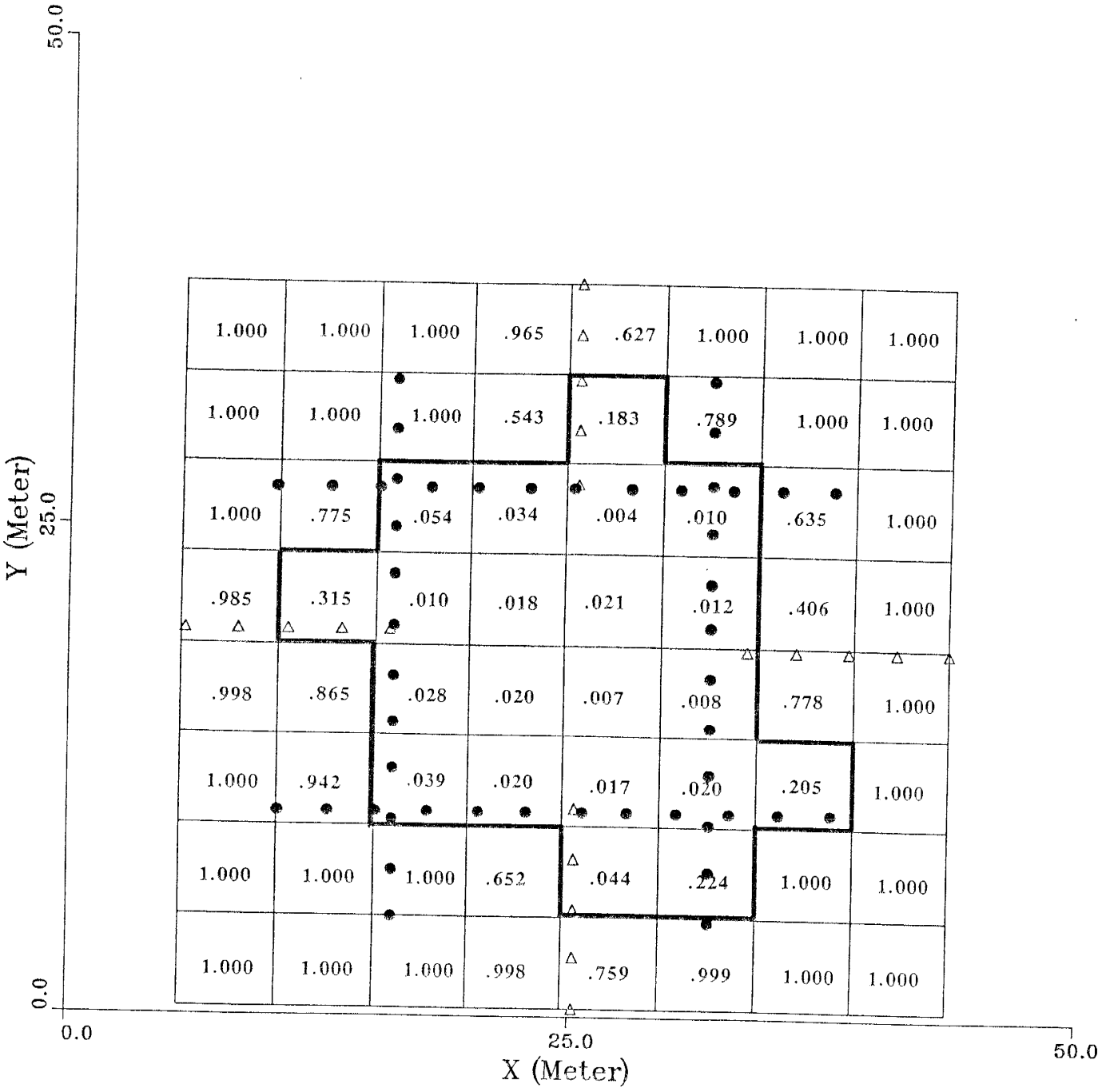

Figure 14. The r_k 's representing the degree of data or model dependent resolution. When $r_k = 1.$, resolution is completely initial model dependent.

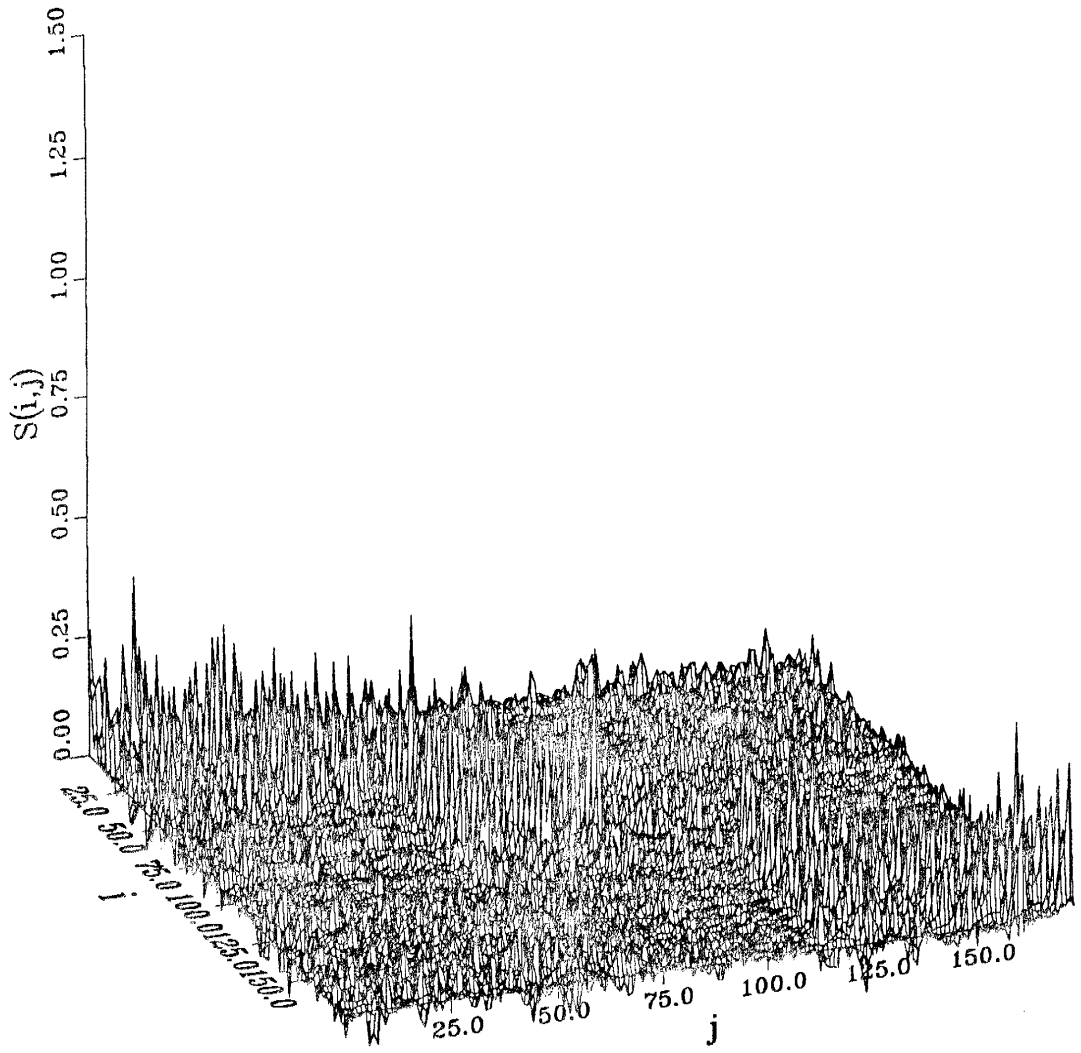

Figure 15. The data resolution kernels. Relatively small amplitudes on the main diagonal are due to large uncertainties of the travel times recorded by the east receiver line.

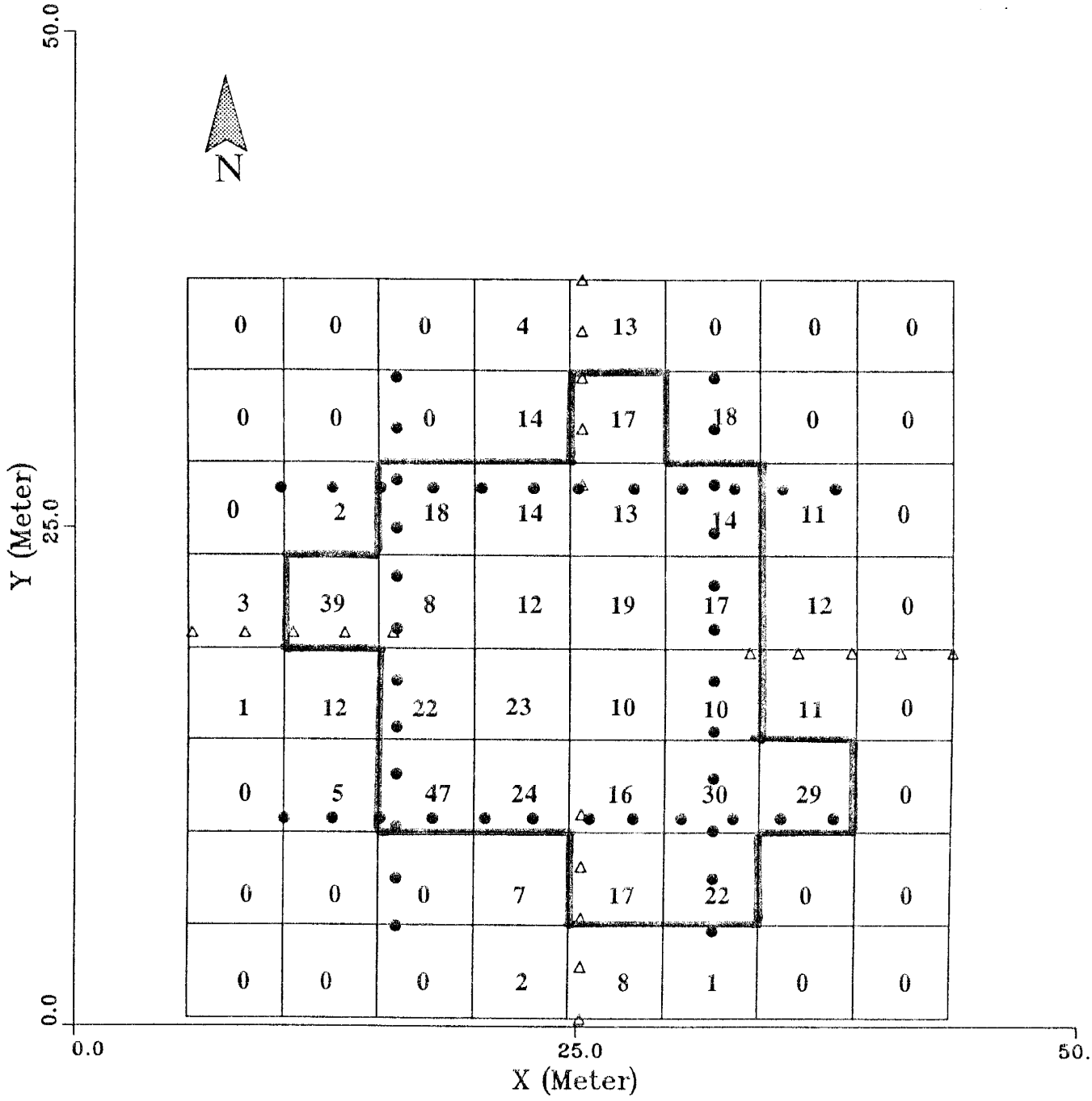

Figure 16. The standard deviations of the resolved parameters in m/s. The cells surrounded by the solid line are resolved mainly data dependent.

Starting with the initial model given in Figure 17, the final velocity model obtained was as shown in Figure 18. The cells which are surrounded by a solid line are mostly resolved by the data. The other cells remaining out of the solid line are the initial model dependent velocities and they should not be taken as *well resolved*.

The low velocity extending from east to west is due to moisture content of the soil which was due to infiltration of the rain water ponded in a pit excavated in the center of the experiment site. However, The cell with ~513 *m/s* which is relatively high at next to the 450 *m/s* contour can not be explained, and this same local high velocity was obtained when all 233 travel times were used (see appendix A). The rays passing through these cells at the seismograms also are much faster than neighboring rays. The relatively high velocity contours corresponds to the unsaturated area of the experiment site.

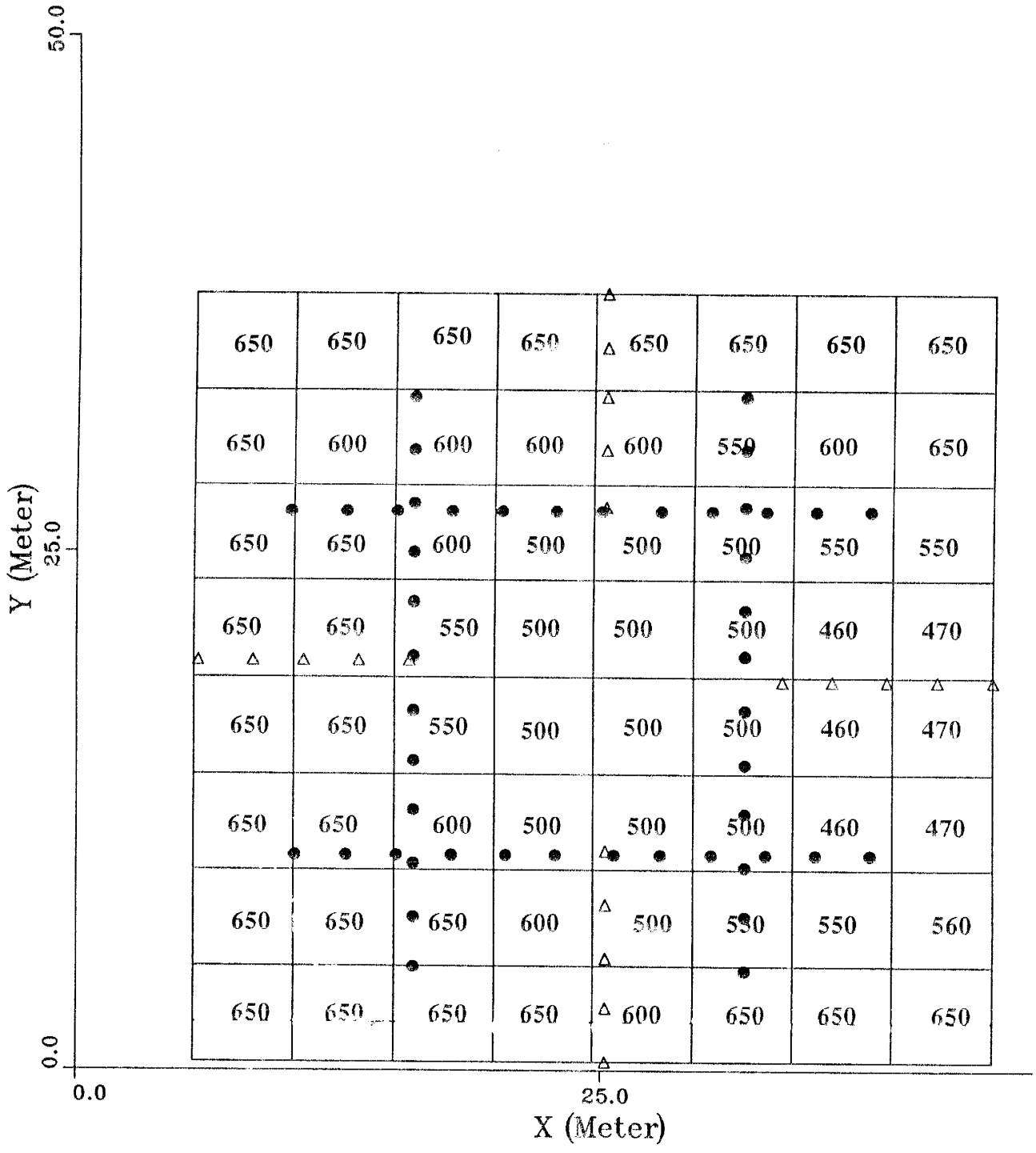

Figure 17. The initial velocity model, values are in m/s.

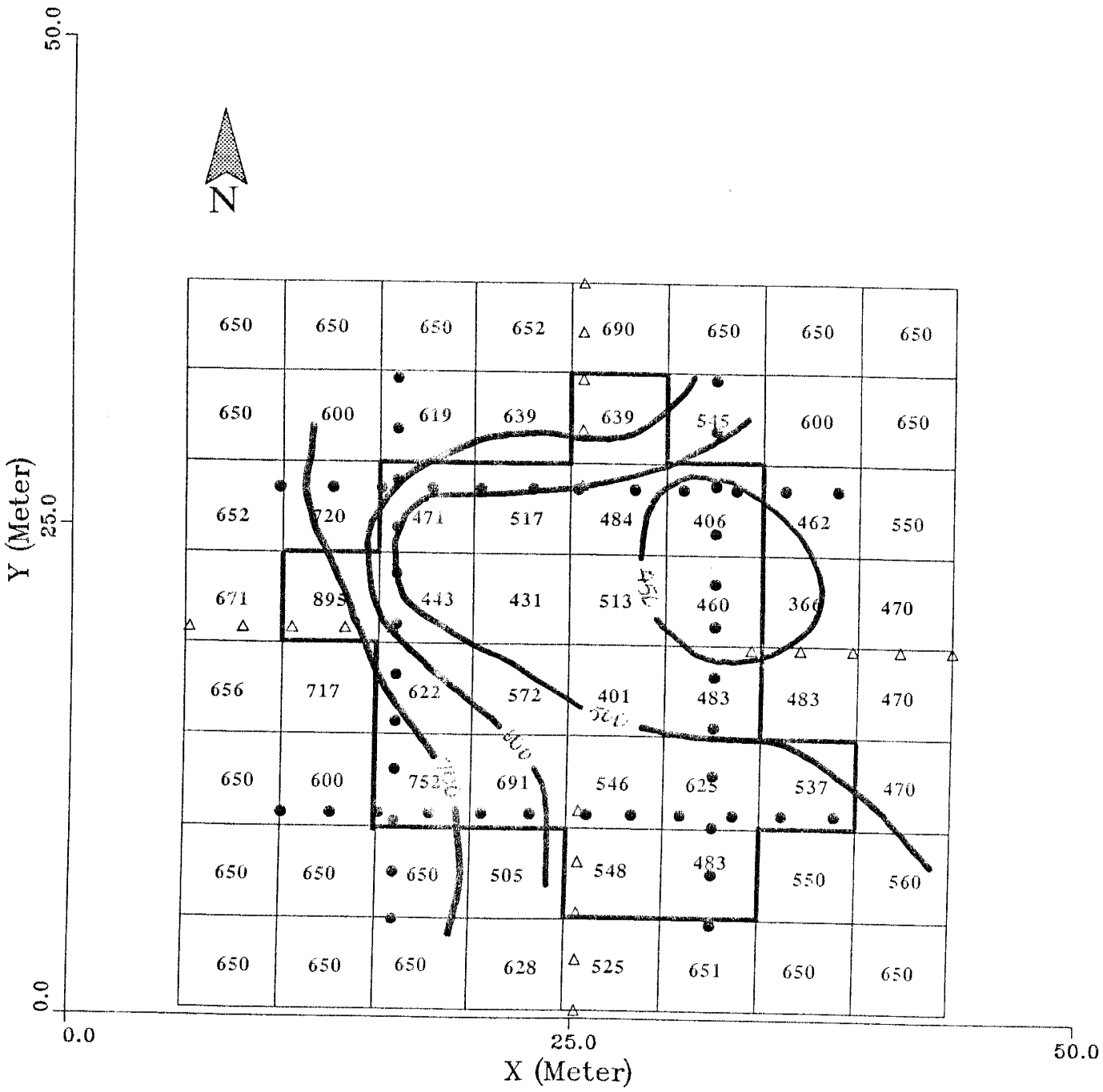

Figure 18. The final velocity model. Values are in m/s. The low velocity extending from east to west is due to moisture content of the soil which was due to infiltration of the water ponded in a pit excavated in the center of the experiment site. The cells surrounded by solid line are mainly data dependent resolved.

6.2. VELOCITY DISTRIBUTION AFTER INFILTRATION

One year after infiltration began, the second data set were collected. The location of the geophones and shots were kept unchanged. The number of travel times collected was 180. The ray paths are not given here because they are the same as given in Figure 9. The same analysis for the velocities of *64* cells was performed as for the first data set (see section 6.1). The **A** matrix in Figure 19 is also very sparse. The vertical axes in meter is the distance that ray *i* travels in cell *j*.If the singular values of the **A** matrix were less than 1.0, they were assumed to be zero (Figure 20).

As given at section 6.1, as well as here, the initial uncertainties were kept the same (Figure 12). A maximum allowable standard deviation of 40 *m/s* was obtained by keeping 25 singular values and associated singular vectors. That is, the degree of freedoms of the data is 25 with condition number 28. 21 of 64 cells were resolved *"uniquely"*, 4 cells were considered resolved because they were only about 30% model dependent which is considered acceptable, and 39 cells where resolved completely from the initial model (see model resolution kernels in Figure 21, and associated $\mathbf{r}_k$'s in Figure 22). The acceptable resolved cells were surrounded by a solid line in Figure 22.

The only apparent differences between the data resolution kernels for the both model seem that some of the travel times recorded by east receiver line, here are being used as much as other travel times (Figure 23). On the other hand same statistical dependency was observed among the rays recorded by the receivers which were located on a same geophone line.

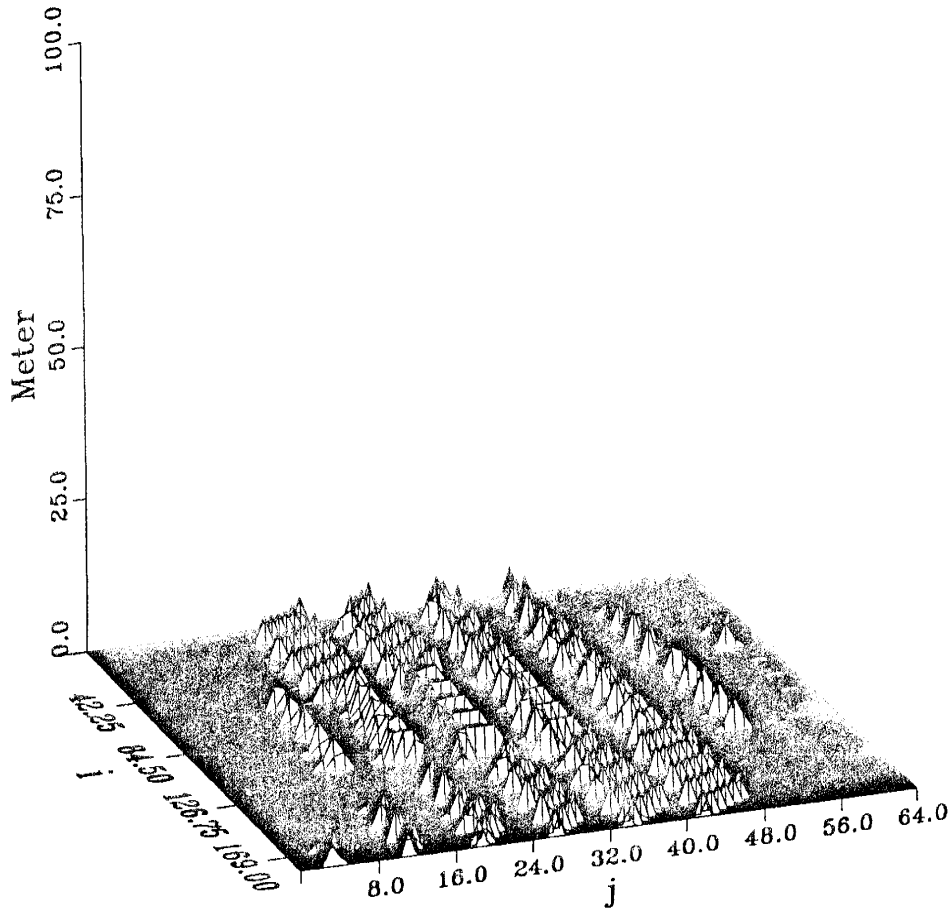

Figure 19. The A matrix. Vertical axes is the distance that ray *i* travels across cell *j* .

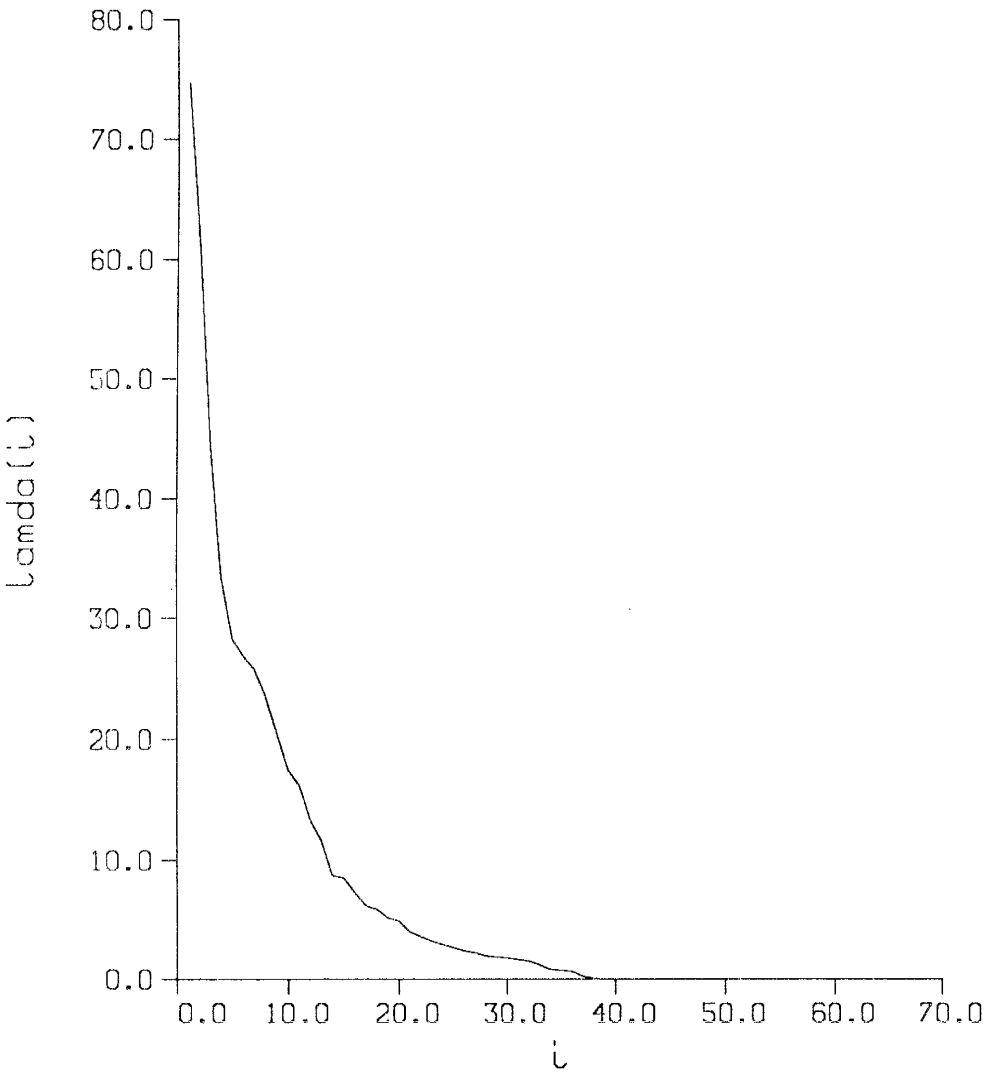

Figure 20. The singular values of the A matrix.

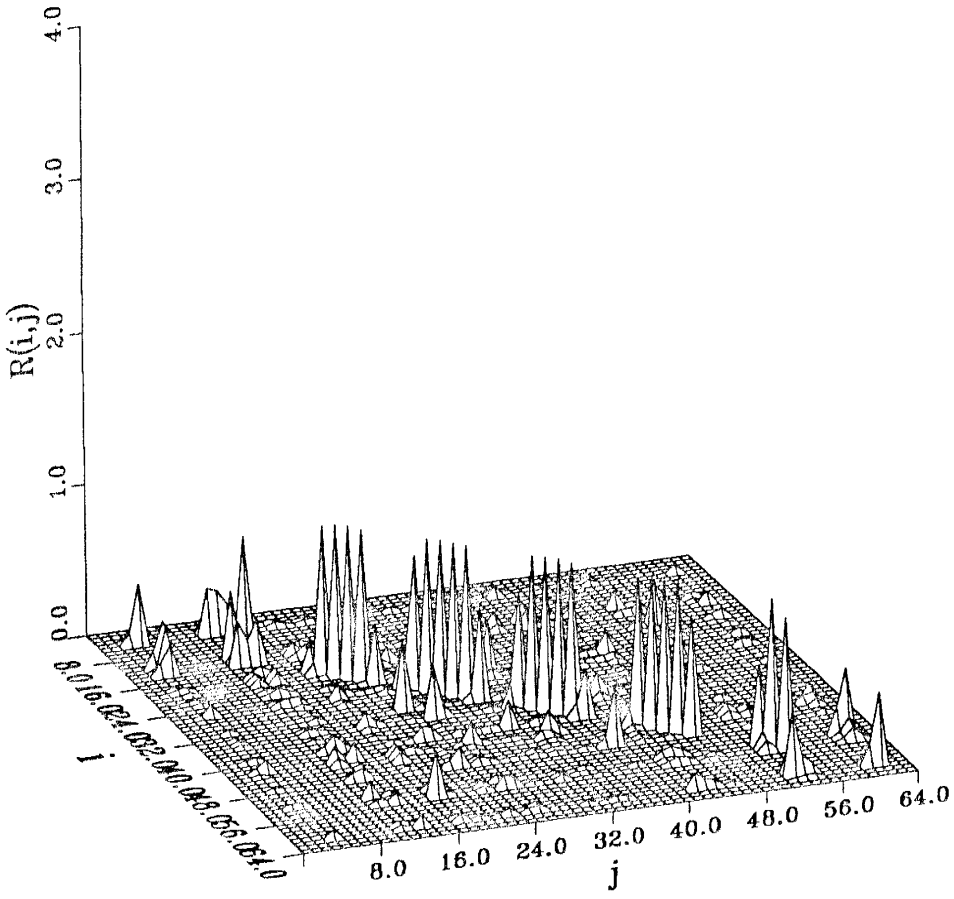

Figure 21. The absolute values of the model resolution kernels. The magnitudes of the diagonal values are the measure of the uniqueness of the associated parameter.

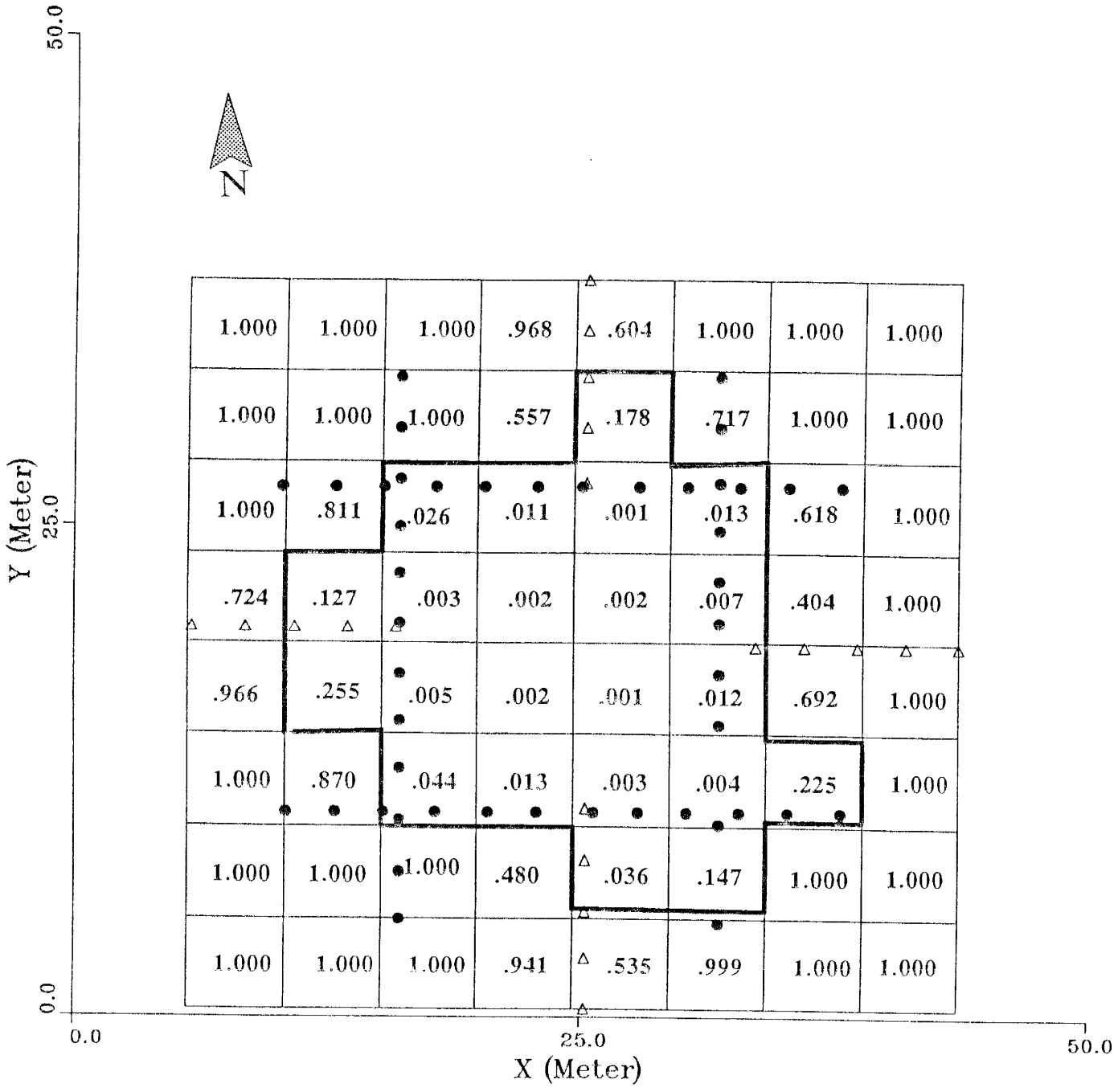

Figure 22. The r_k 's representing the degree of model or data dependent resolution.

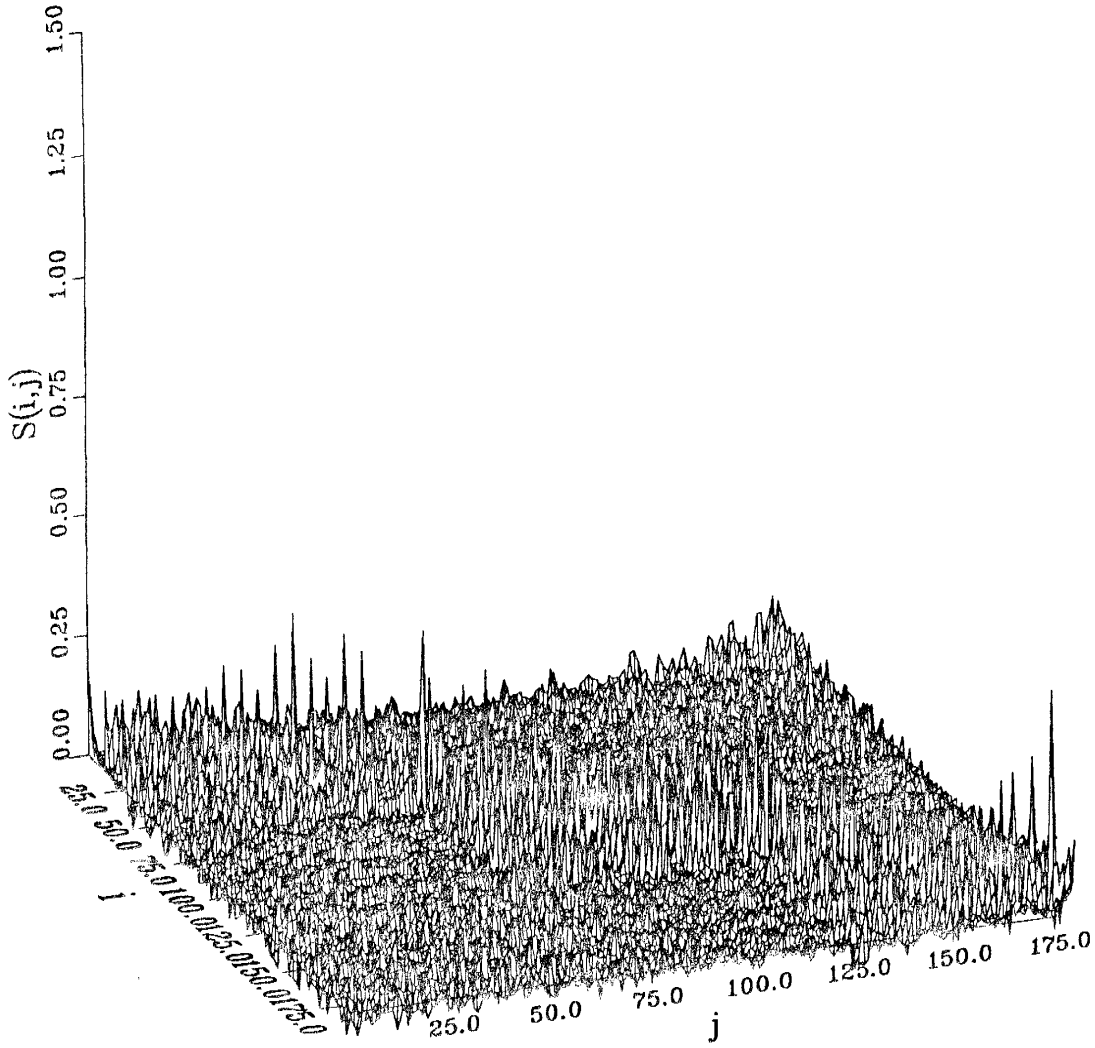

Figure 23. The data resolution kernels.

The standard deviations, in meters per second, for the cells are given in Figure 24. As mentioned earlier zero standard deviations are for cells whose velocities are totally dictated by the initial model. The cells within solid line are the cells which resolved either uniquely or less than %30 model dependent.

When two different initial modes are used, the source of distortion occurs in final residual velocity in existence of non-unique solution. Therefore the initial model given in Figure 17 was kept the same for this model despite *bad fit* or improper scalar R.

The characteristic of the final velocity model (Figure 26) is that 450 m/s contour in Figure 18 was replaced by 400 *m/s* in expanded form after infiltration began. High velocity contours obtained before infiltration ,here, expanded mainly through south-west direction. The two cells near to the 450 *m/s* contour in Figure 18 with relatively high velocity, without any explanation remained relatively high as well.

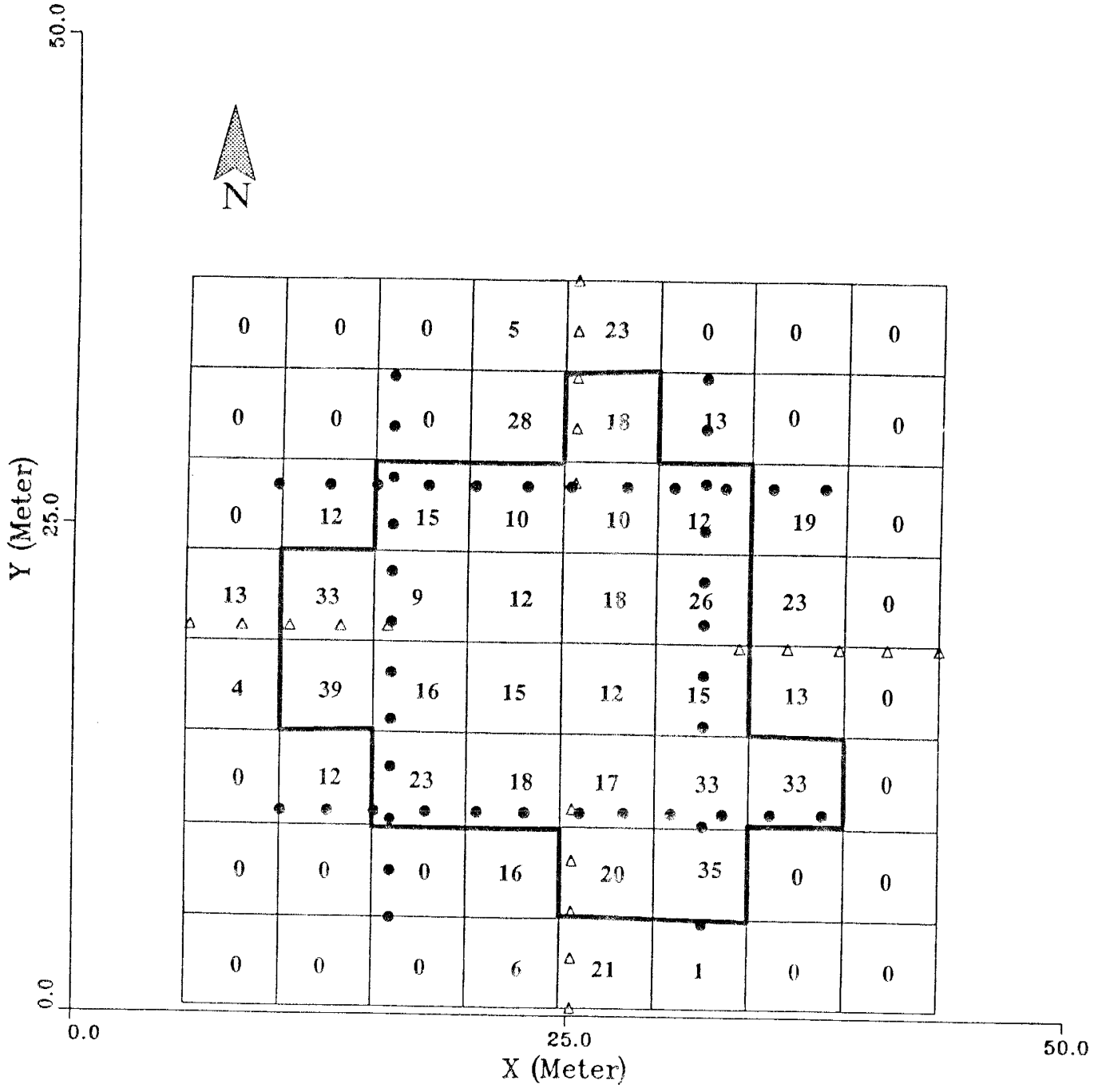

Figure 24. The standard deviations (in m/s) of the final velocity model. Zero standard deviations are due to initial model dependency only. Good enough resolved cells are surrounded by solid line.

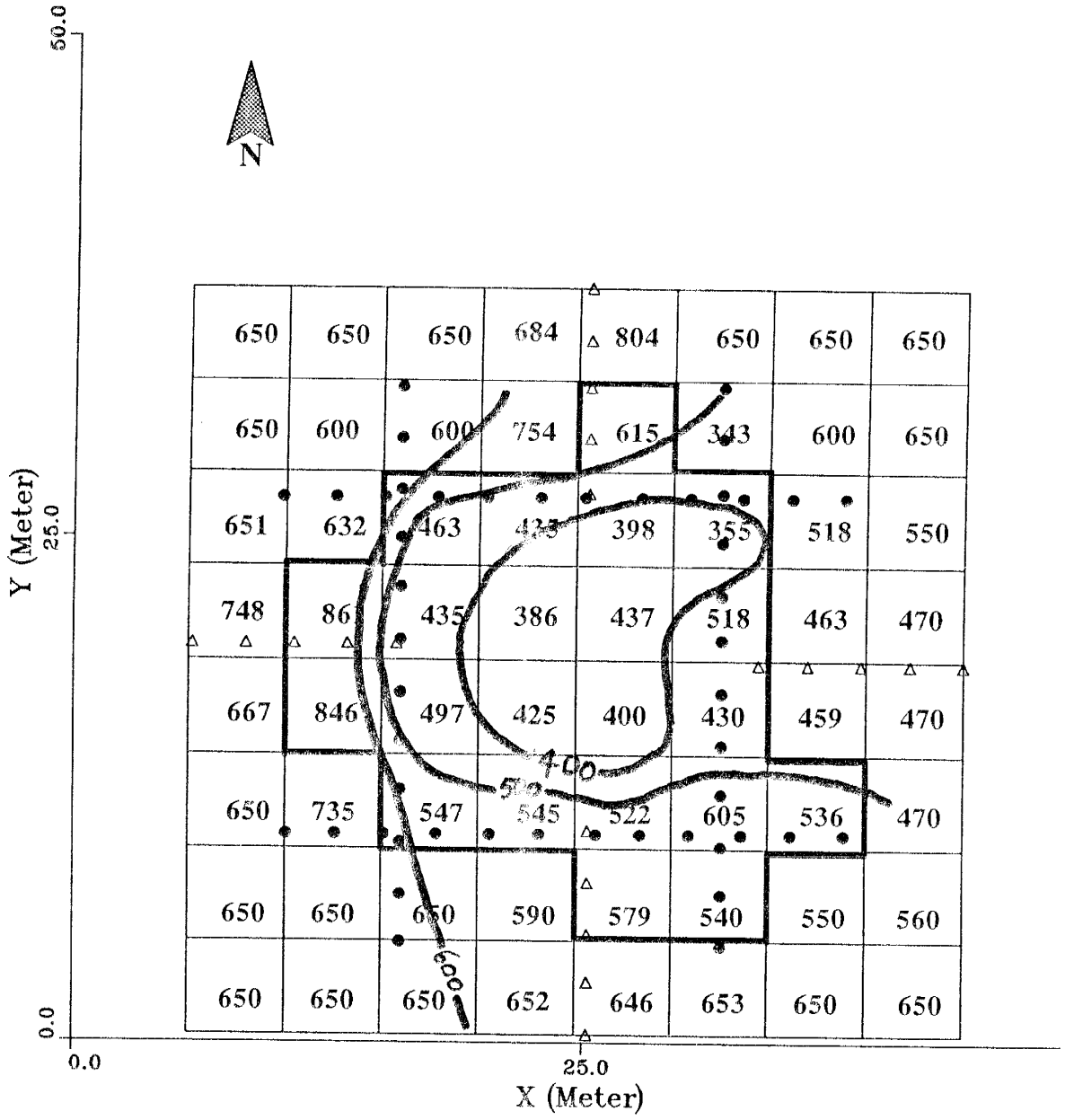

Figure 25. The final velocity model in m/s. The cells resolved mainly by the data are surrounded by solid line. One year after infiltration began, the contours start extending basically through southwest direction. Since the seismic coverage at east and northeast was poor the continuation of the contours clearly can not be seen.

7. RESULTS

The residual velocity distribution caused by infiltration is given in Figure 26. The shaded areas in the figure are the cells which resolved by both data set, before and after infiltration. The contour values are in m/s. The lateral pathway is basically through north-east and south-west direction. Direct hydraulic measurements in the experiment site also yielded the parallel results(see Parsons, 1988).

Since the residuals represent the differences between the velocity in 1987 and velocity in 1986, the standard deviations for the residuals can be written in terms of both standard deviations *(Meyer L.S.,1975)* of final models as:

$$\sigma_{res} = [\ \sigma_{1987}^2 + \sigma_{1986}^2\ ]^{1/2}$$

The vertical and horizontal sections of Figure 26 are plotted in Figure 27, so that decreasing in velocity can be compared for every cell with its associated double standard deviations.

Travel time of the seepage also can be calculated for a given direction if enough number of set of data were available. Only two data set obviously are not proper to make such a decision.

Several boreholes (more than 20) at the experiment site were drilled for the instrumentation to determine the wetting front locations and rates of advance of wetting front in an expensive way. However, if proper shot-receiver configurations are used, the travel time and pathway of seepage can be determined by determining a discrepancy in seismic wave velocity in time.

Under the condition of high rate of precipitation, the results are about to be interpreted together with precipitation records. In the same way, in arid and or semi-arid environment, the rate of evaporation may cause a difficulty in determining the wetting front and penetration velocity.

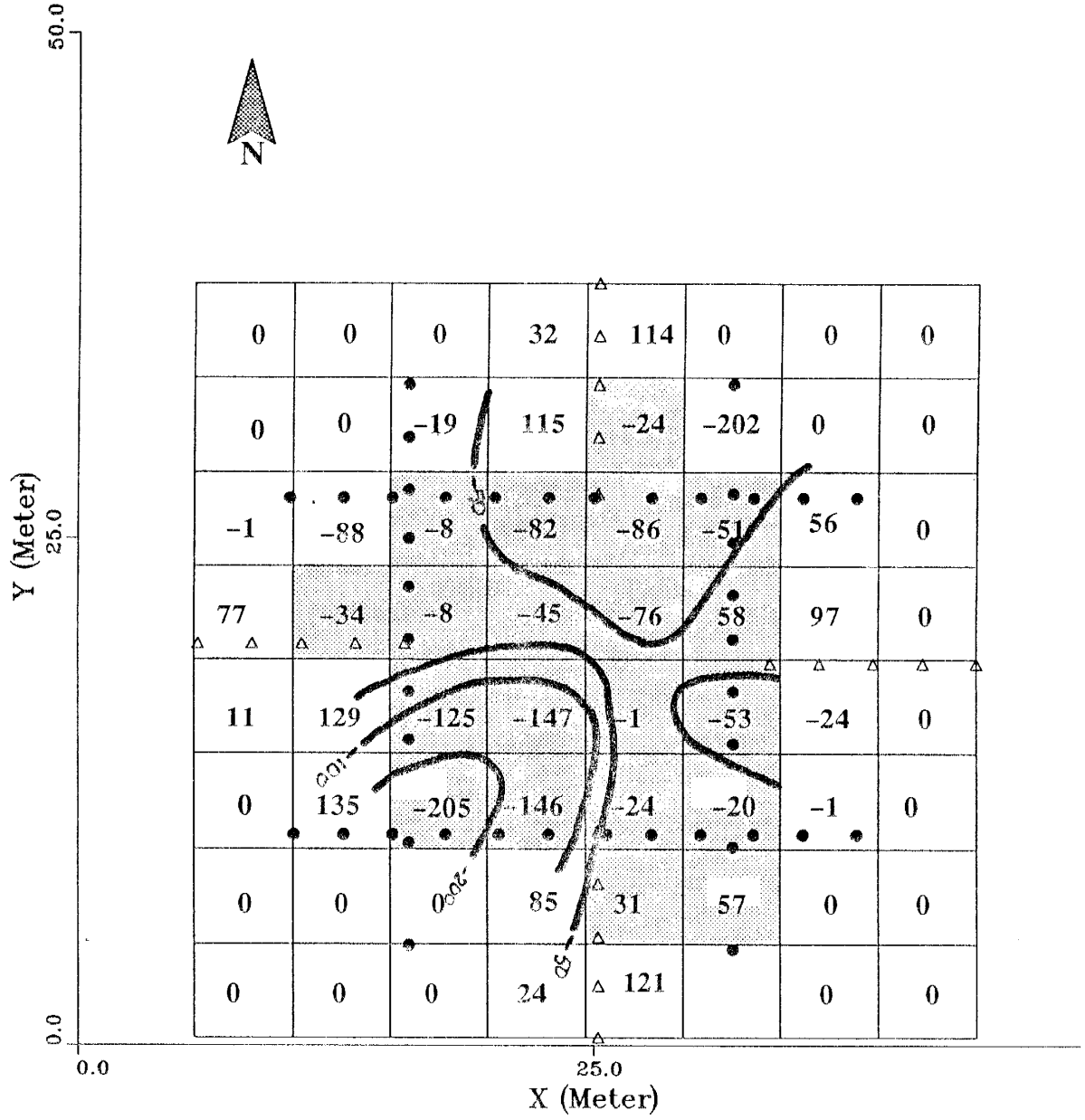

Figure 26. The changing in velocity due to the infiltration within one year (values are in m/s) and penetration direction. Due to low seismic coverage at the east, the continuations of the contour values are not clear.

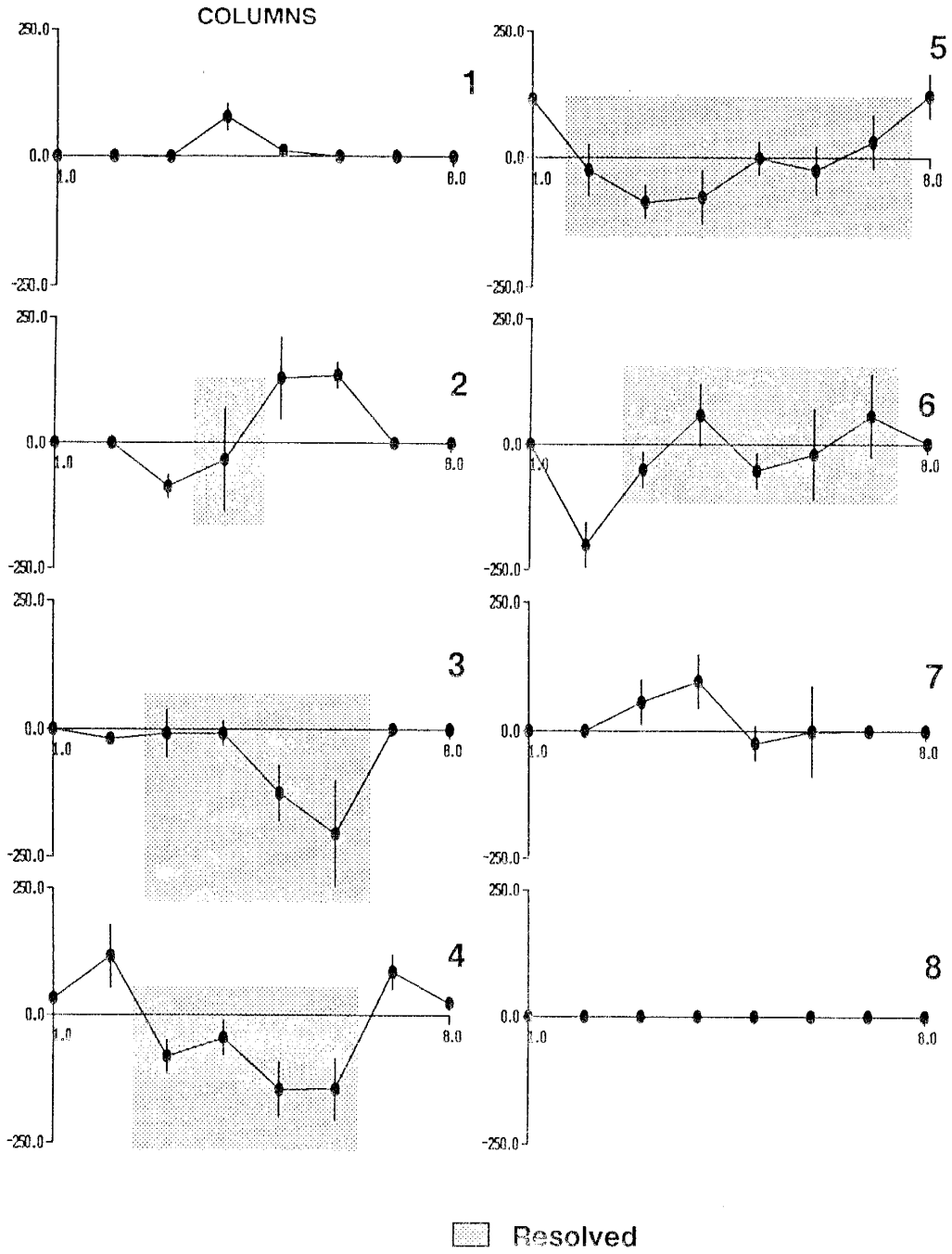

Figure 27. The vertical profiles taken from Figure 24 associated with doubled standard deviations.

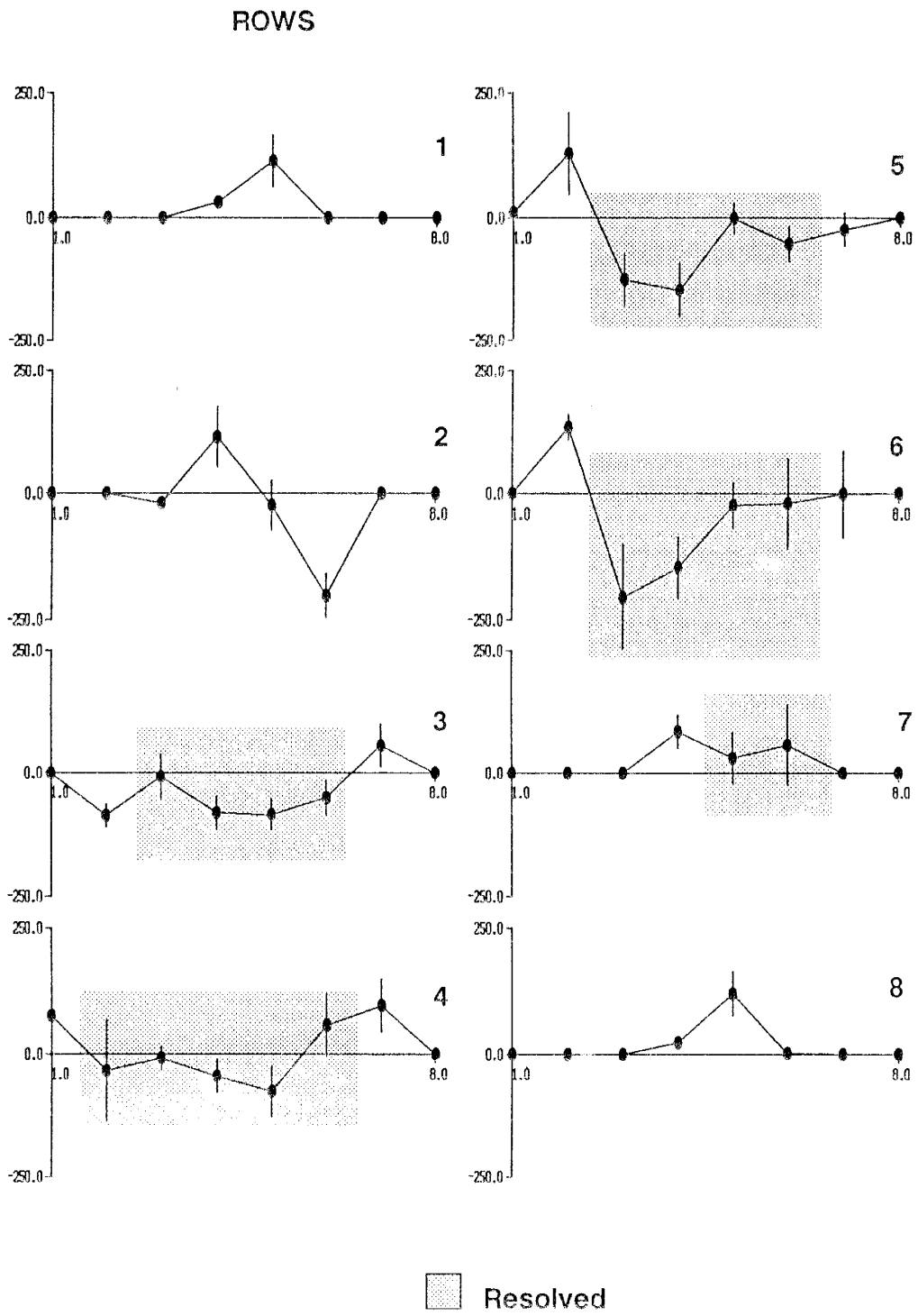

Figure 27 (CONTINUE). The horizontal profiles taken from Figure 24 associated with doubled standard deviations.

8. DISCUSSION

The idea of using cells in obtaining velocity distribution within the second layer is an approximation. The calculated velocity for each individual cell represents itself an average. In other words the velocity of one cell is influenced by the average velocity of neighboring cells. The size of the cells, therefore, become very important in prescribing a desired resolution. Changing in the size of cells act as a moving average operator in this type of problem. The minimum wavelength, in fact, I tried to capture in this problem is not smaller than five meter. Using *8x8=64* cells in squared shape than resulted capturing at least five meter wavelength of changing in average. If the size of the cells were different in both model proposed earlier, the comparison between these two models would have been difficult even wrong. The reason of this is that both of final models would have contained different wavelength content. As a result, keeping the size of the cells same in time is as same as keeping the wavelength content unchanged.

The assumption of ignoring the delay times in both model yields not the real velocity but relative velocity distribution in space. Since the delay times influence both data set systematically as assumed, the residual velocity distribution in time is not effected by this assumption.

The important assumption of the inversion algorithm used in this study is that data are assumed to be statistically independent, or degree of independence theoretically is assumed to be high. However, in real world, it is sometimes impossible to collect such data. For example, two rays traveling on same geometric plane are more dependent than rays traveling on different geometric planes. The rays leaving from the same shot lines as shown in the data resolution kernels seem they are not independent. The

cells, resolved only by these rays were calculated as combinations of each other. The rays, on the other hand, leaving from different shot points are mainly independent. Therefore, the cells resolved by these rays are resolved uniquely.

The *good enough* initial velocity model of the first data set was obtained by use of prior information; starting with low velocities at the center of the experiment site because of previous moisture content and high velocities at the surrounding areas. The *"goodness–of–fit"* or the scalar R for the first model was calculated to be 3.68 . The initial model, therefore, seem it was chosen *"poorly"*. On the other hand, the best fit at the final model were R=0.96. That is, the parameterization was complex enough for the first model if the uncertainties of the travel times where chosen properly.

When one deals with large size of matrices, the major difficulties are in computing, storage, as well as round off error. Significant round off error was observed in calculating the distances which rays travel within individual cells. Similar problems aroused in decomposing the **A** matrix. In order to overcome these problems entire calculations were performed in doubl precision.

The residual velocity distribution would be modeled by only taking the residuals between both travel time data set. However, standard deviations of final residual velocities, in this way, are not still independent of velocities distribution before and after infiltration. Therefore, setting up the two models was necessary.

The assumption of straight ray paths in this problem was reasonable because of the short distances. However, ray bending or curvature in long distances would be much more effective that straight ray path assump-

tion may not work at all. A detailed discussion dealing with ray curvature and supported by artificial tomographic models is given by *Dyer B.,Wothington M.H.,1988.*

The infiltration within one year caused approximately 50 to 150 m/s decrease in velocity. The decreases were observed where unsaturated structure use to exist. The moisture content at the center of the experiment site caused less decrease in velocity after infiltration. On the other hand the unsaturated material with relatively high velocity, after infiltration responded quite low velocity. Despite the assumptions and their implications, the final results were obtained reasonable.

9. CONCLUSION

Predicting lateral and/or downward pathway and travel time for seepage through unsaturated material can be accomplished by following a changes in time in seismic wave velocity with time. Tomographic determination, in this type of problem can successfully be used in obtaining behavior of multidimensional flow. The greatest source of distortion in residual velocity distribution may occur where a high rate of natural precipitation exists. However, in arid or semi-arid climate the effect of precipitation on seismic wave velocity are probably low and can be ignored.

REFERENCES

Bishop,T.N.,et al., 1985, *Tomographic determination of velocity and depth in laterally varying media:* Geophysics, **50**, *903–923.*

Chiu, K.L.S., and Stewart, R.R., 1987, *Tomographic determination of three dimensional seismic wave velocity structure using well logs, vertical seismic profiles, and surface seismic data*: Geophysics, **52**, *1085–1098.*

Cottin,J.F. et al., 1986, *Curved ray seismic tomography: Application to the Grand Dam (Reunion Island):* First break, **4**, no.2, *25–30.*

Crosby,J.W., Johnstone, D.L., Drake, C.H., and Fenton, R.C., 1968, *Migration of pollutants in a glacial outwash environment*: Water Resour. Res., **4(5)**, 1095–1114

Crosby,J.W., Johnstone, D.L. and Fenton, 1971, *Migration of pollutants in a glacial outwash environment 2.* : Water Resour. Res., **7(1)**, 204–208.

Dines,K.A., and Lytle,R.J., 1979, *Computerized geophysical tomography:* Proc. Inst. Electr. and Electron. Eng., **67**, *1065–1073.*

Dyer, B.,Worthington, M.H., 1988, *Some sources of distortion in tomographic velocity images:* Geophysical Prospecting, **36**, *209–222.*

Gustavsson,M.,Ivanson,S.,et al., 1986, *Seismic borehole tomography– Measurement systems and field studies:* Proc. Inst. Electr. Electron. Eng., **74**, *339–346.*

Ivanson, S., 1985, *A study of methods for tomographic velocity estimation in the presence of low velocity zones*: Geophysics, **50**, *969–988*

Ivanson,S., 1986, *Seismic borehole tomography– Theory and computational methods:* Proc. Inst. Electr. Electron. Eng., **74**, *328–338.*

Jackson, D.D., 1972, *Interpretation of inaccurate, insufficient and inconsistent data: Geophy. J. ast. Soc.*, **28**, *97–109*

McMechan, G.A., 1983, *Seismic tomography in boreholes:* Geophys. J. Roy.Astr. Soc., **74**, *601–612.*

Menke, W., 1984, Geophysical Inverse Theory

Menke, W., 1984, *The resolving power of cross-borehole tomography:* Geophys. Res. Lett., **11**, *105–108*

Miller, D.E., and Gardner, W,H., 1962, *Water infiltration into stratified soil*: Soil Sci. Soc. Am. J., **26**, 115–118.

Mualem, Y.,1984, *Soil anisotropy of unsaturated soils*: Soil Sci. Soc. Am. J., **48**, 505–509

Palmquist, W.N., Johnson, A.I., 1962, *Vados flow in layered and non layered materials*: USGS Pfof.Paper, **450–C**, C142–C143.

Peterson,J.E., *et. al.*, 1985, *Applications of algebraic reconstruction techniques to crosshole seismic data:* Geophysics, **50**, *1566–1580.*

Parsons, A.M., 1988, *Field simulation of waste impoundment seepage in the vadose zone: Site characterization and one dimensional analytical modeling* : Master Thesis,New Mexico Institute of Mining and Technology.

Ramirez, A.L., 1986, *Recent experiments using geophysical tomography in fractured granite:* Proc. Inst. Electr. Electron. Eng., **74**, *347–452.*

Richard, L.B., Faires, J.D., 1984, *Numerical analysis, third ed., PWS publications, pp: 440.*

Schlue, J.W., Singer, P.J., Edwards, C.L., 1986, *Shear wave structure of the upper crust of Albuquerque – Belen basin from Rayleigh wave phase velocities: GGR,* **91**, *6277–6281.*

Schlue, J.W., Hostettler, K.K., Edwards, C.L., 1987, *Evidence from Rayleigh Wave Data for Magma in Upper Crustal Dike In Albequerque – Belen Basin of the Rio Grande Rift, New Mexico*: GGR, **92**, No.B9, *9281–9292.*

Schlue, J.W., 1988, *Personal communication, Proffessor of Geophysics, New Mexico Tech, Socorro, NM, 87801.*

Stephen,K.L.C., Stewart,R.R., 1987, *Tomographic determination of three dimensional seismic velocity structure using well logs, Vertical Seismic Profiles and surface seismic data:* Geophysics, **52**, *1085–1098.*

Stewart,R.R., 1985, *Seismic tomography: Pursuing a better subsurface picture:* Oilweek, **9**, *21–24.*

Stephens, D.B., and Heerman, 1988, *Dependence of anisotropy on saturation in a stratified sand*: Water Resour. Res., **24(5)**, 770–778

Tien-When Lo, *et.al.*, 1988, *Ultrasonic Laboratory tests of geophysical tomographic reconstruction:* Geophysics, **53**, *947–956.*

Treitel, S., Lines, L.R.,1988, *Geophysical examples of inversion (with a grain of salt): The Leading Edge*, **7**, *32–35*

Wiggins, R.A., Larner, K.L., Wisecup, R.P., 1976, *Residual static analysis as general linear inverse problem:* Geophysics, **41**, *922–938.*

Worthington, M.H., 1984, *An introduction to geophysical tomography:* First Break, **2**, *20–26.*

Yeh, J.T.C., and Gelhar, L., 1983, *Unsaturated zone in heterogeneous soils in the Role of the Unsaturated zone in radioactive and hazardous waste disposals*, Ed. Mercer J.W., and others, Ann Arbor Science, Ann Arbor, MI.

APPENDIX A

The analysis for the first data set with its *233* travel times was performed in this section. Because of inconvenient size of the matrixes, they are not given here. In order to obtain a best fit to the data various model has been tested; at final *11x11=121* cells were chosen as the model. The equation system solved here contains *233* observation with *121* unknown velocity. This large size of the equation system required hours of computing time.

The degree of freedom of the data, with *40 m/s* maximum tolerable uncertainty were obtained *34* with condition number *10*. When *34* singular values and their associated singular vectors are kept, the $\mathbf{r}_k$'s corresponding to the cells are given in Figure A1. *23* of the cells were resolved *"uniquely"*, and 10 of the cells were resolved less than *30%* model dependent. The cells which resolved *" acceptable"* and/or *"uniquely"* were marked in the Figure by solid line.

Associated standard deviations for each cells are given in Figure A2 in *m/s*. The zero uncertainties are due to the resolution from the initial model only. Initial uncertainties (τ_j) in m/s are given in Figure A3. Since the size of the cells are very small (~ 3. meter) in compare to the model given in **6.1** the difficulty aroused in designing the initial model and associated uncertainties. This is because local velocity anomalies become much more effective. Therefore, *80 m/s* initial uncertainty used for previous models, here was replaced by *100 m/s* instead.

The initial model with scalar R = 5.83 is given in Figure A4. Poorly estimated this initial model may be unacceptable. On the other hand, when one considers the size of the equation system of which each calculation takes hours of computing time, the better initial could have not been obtained. However, the *"goodness-of-fit"* for the final model with R=1.107 is acceptable good. The final *"complex enough"* chosen model is given in Figure A5. The contour values given in the figure are in *m/s*. The contours in this model shows nearly the same pattern as obtained in **6.1.**

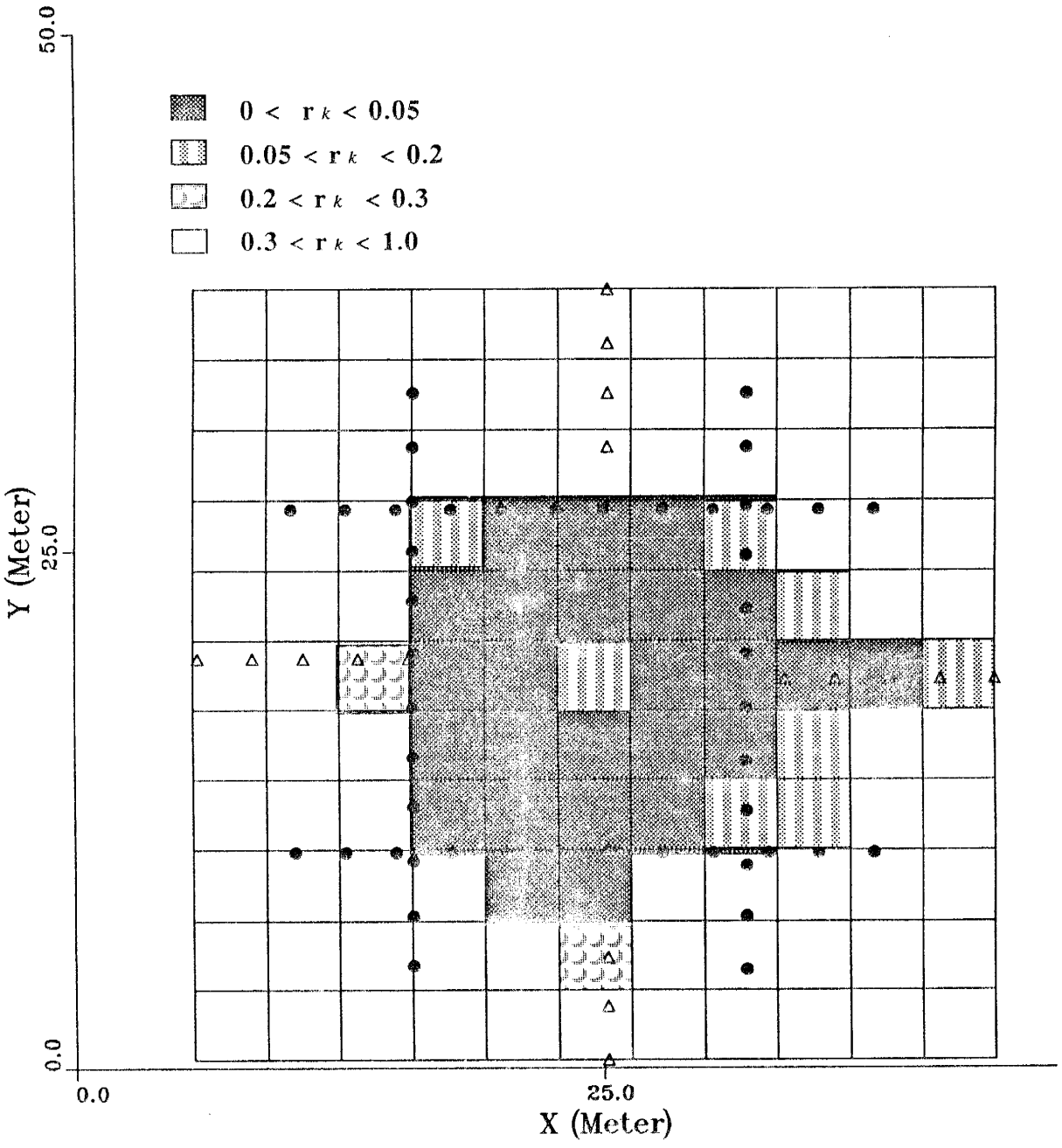

Figure A1. The r_k 's

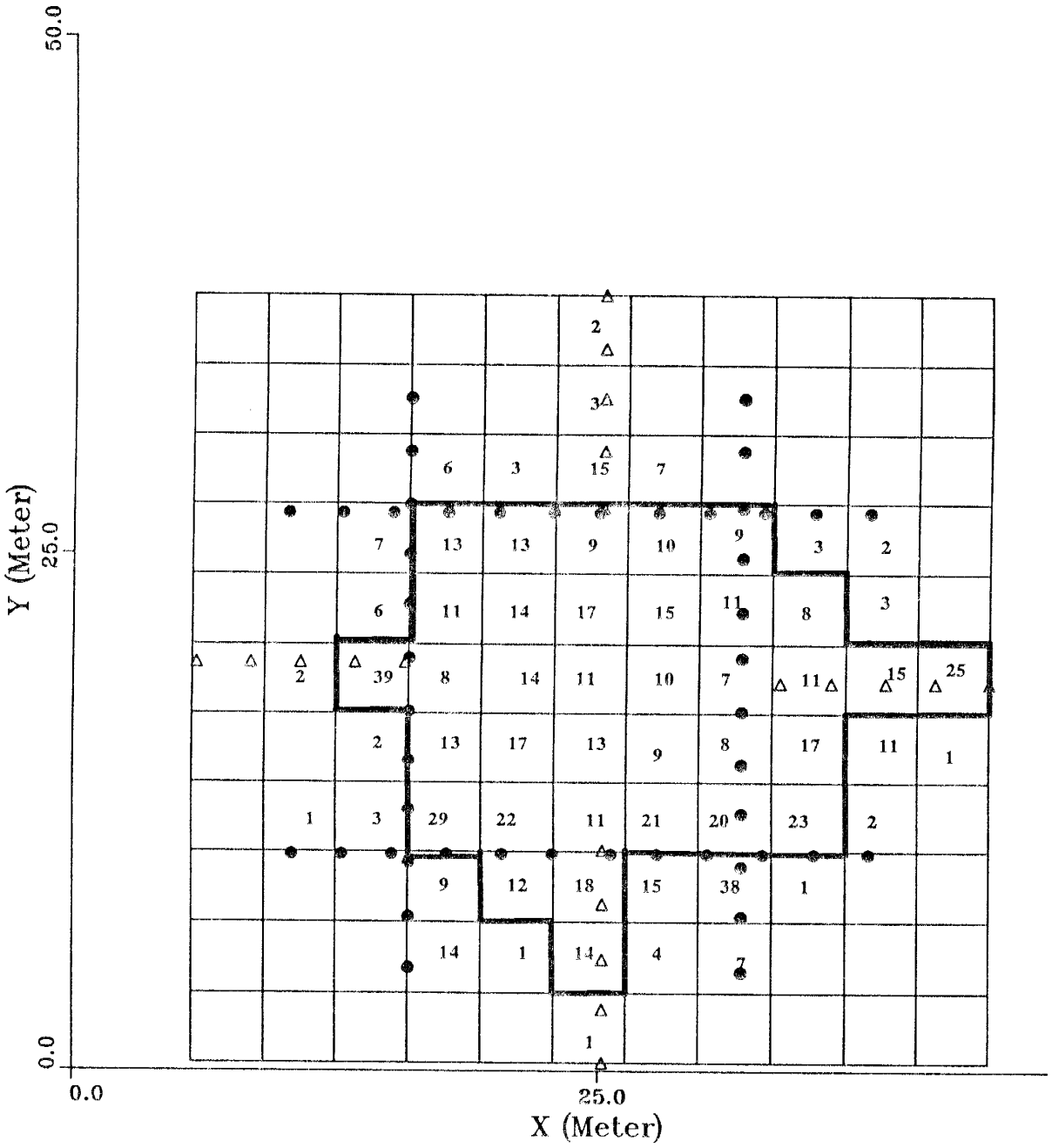

Figure A2. The standard deviations of the resolved parameters in meter per second.

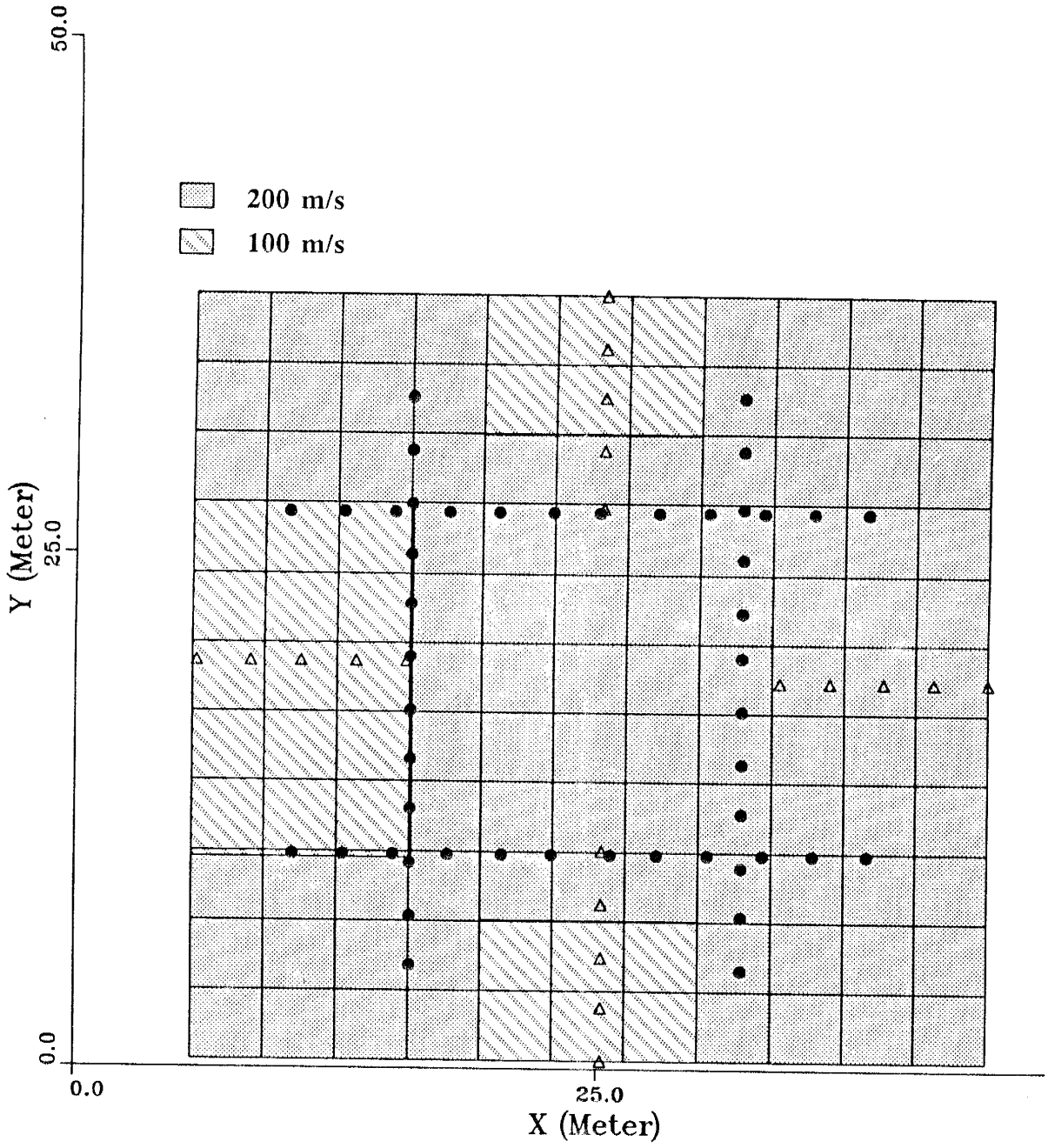

Figure A3. The initial Uncertainties (τ_j)in meter/second.

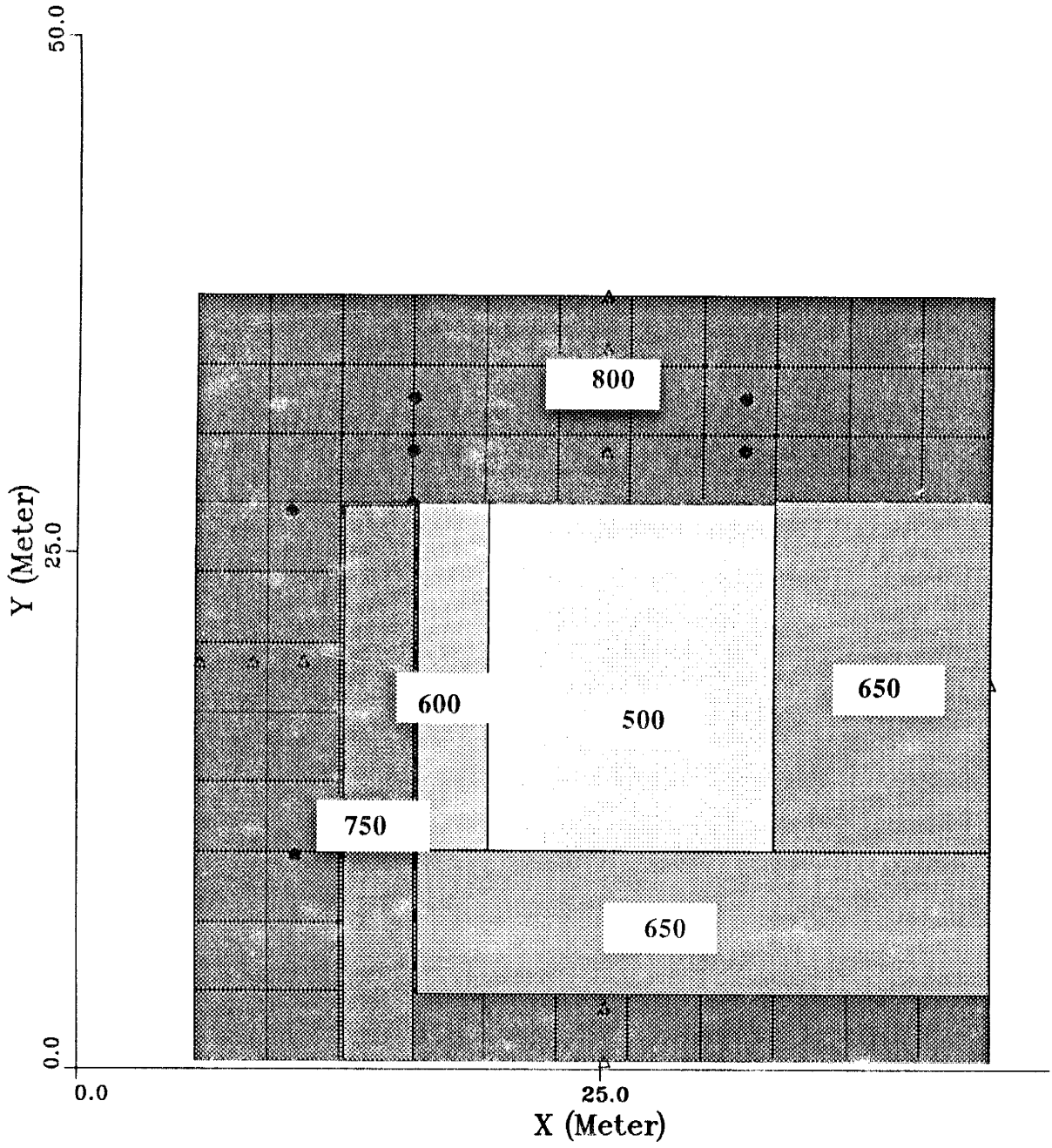

Figure A4. The Initial model. Velocities are in meter/second.

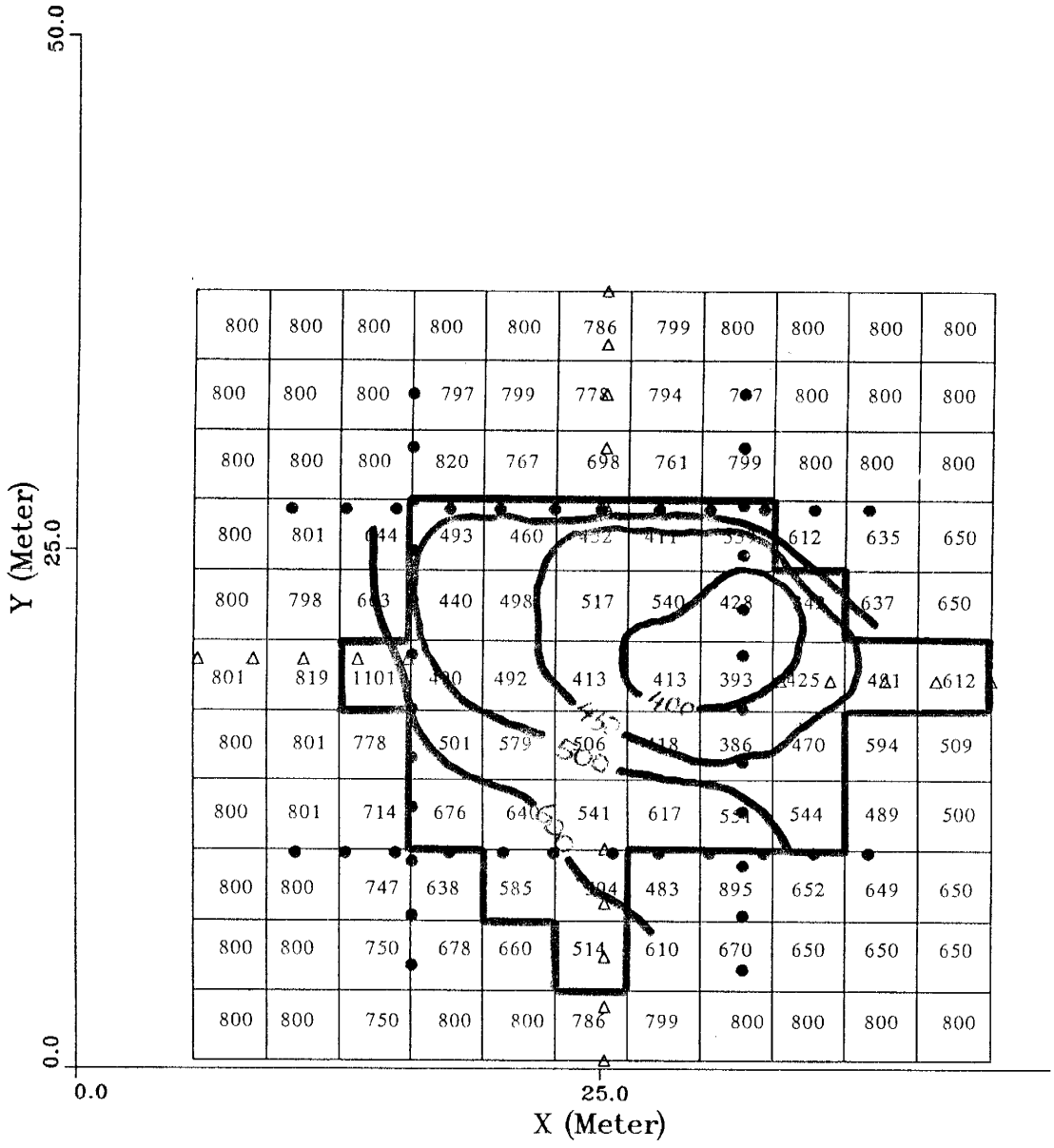

Figure A5. The final velocity model in meter/second.

APPENDIX B

```
C-------------------------------------------------------------
C          THIS PROGRAM SOLVES ANY LINEAR SYSTEM GIVEN AS
C                (Y - YTH)  =  A * (X - X0)
C          or      DELTA (Y)  =  A * DELTA (X)
C     ALSO CALCULATES THE Uncertainties FOR EACH PARAMETER BY
C         MEANS OF Uncertainties OF THE OBSERVED DATA
C     IF Uncertainties OF SOME PARAMETER IS KNOWN PROGRAM THEN
C     WORKS MAINLY FROM INITIAL MODEL INSTEAD OF DATA
C          UNDER AND OVER CONSTRAINT CASES ARE BEING CONTROLLED
C          BY THE PROGRAM ITSELF. NO CHANGING IS Necessary
C          IN THE PROGRAM TO DO SO.
C              ******   IMPORTANT  ******
C          DELTA(Y), MATRIX A, DELTA(X) ARE INPUT
C
C
C REFERENCE:
C       Jackson,D.,D.,1972,Interpretation of Inaccurate, Insufficient
C              and Inconsistent Data.,Geophys.J.astr.Soc,28,97-109
C-------------------------------------------------------------
C          Written by :    Abdullah Karaman
C                          September 1, 1988
C
C                 Revised :              September 8 ,1988
C                   Revised for uncertainty: September 11,1988
C                   Revised for Decomposition: September 27,1988
C                   Revised for Quantity rk  : October 6,1988
C                   Revised for Scalar R  : October 10,1988
C-------------------------------------------------------------
                  program lanczosinvers
                  common /worksp/dwksp
C   if uncertainty .eq. 0.0 , define 'uncertainity = epsilon'
C
C       thus avoid division by zero
C       ICODE AND LCODE WERE EXPLAINED AT THE NEXT LINES
C-------------------------------------------------------------
C   CNANGEABLE PARAMETERS ( USER DEPENDENT)
C-------------------------------------------------------------
      parameter (ndim=250,epsilon=1.0d-003,infinit=999999)
C-------------------------------------------------------------
C   DO NOT CHANGE THE FOLLOWING PARAMETERS !....
C-------------------------------------------------------------
      parameter (zero=0.0d+00,one=1.0d+00,ICODE=1,LCODE=11)
      parameter (intzero=0,intone=1,inttwo=2,two=2.00d+00)
                character*1 ncode
                character*20 namein,nameout
       real dwksp(200000)
       double precision tmpr,rscalar,residual,reciprocal,rqscalar,
     ! sumj,sumi,delta
      double precision x(ndim),a(ndim,ndim),y(ndim),p(ndim),s(ndim),
     ! ydelta(ndim),yth(ndim), pcalc(ndim),uncy(ndim),uncp(ndim),
     ! u(ndim,ndim),v(ndim,ndim),ve(ndim,ndim),vve(ndim,ndim),
     ! vveu(ndim,ndim),rk(ndim),sm(ndim,ndim),rm(ndim,ndim),
     ! ycalc(ndim),ahold(ndim,ndim),punc(ndim)
       integer q
       CALL IWKIN(200000)
C-------------------------------------------------------------
C   INPUT AND OUTPUT FILE PREPARATION
C   WHEN ncode = "t"  OUTPUT FILE IS NOT CREATED
C-------------------------------------------------------------
      write(6,*)'Input file : ? '
      read(5,*)namein
      write(6,*)'Where you want me to write the output ?'
      write(6,*)'For terminal enter 't',any character otherwise '
            read(5,*)ncode
            if(ncode.eq.'t')go to 10
            nwrite=2
```

```
            write(6,*)'Output file : ? '
            read(5,*)nameout
      open(unit=nwrite,file=nameout,status="new")
            go to 20
 10         nwrite=6
 20         continue

C-------------------------------------------------------------
C     OPENING INPUT FILE
C-------------------------------------------------------------

      open(unit=9,file=namein,status="old")

C-------------------------------------------------------------
C     THE INPUTS :
C     y(i),i=1,2,...ndat  : Observations at x(i)
C     uncy(i),i=1,..ndat  : Uncertainitise of y(i)
C     yth(i),i=1,2,...ndat  : Theorethical y(i) at x(i)
C     P(i),i=1,mpar   : Initial values of model parameters.
c     kstep : step size when ignoring the eigen values
C-------------------------------------------------------------

            read(9,*)ndat,mpar,kstep,kto,tol

c.. CHECK IF # OF OBSERVATIONS OR # OF PARAMETERS
C..   ARE BIGGER THAN  AVALIABLE ARRAY
            if(ndat.gt.ndim.or.mpar.gt.ndim)go to 999

c..OBSERVED AS INPUT
            read(9,*)(y(i),uncy(i),i=1,ndat)
            read(9,*)(x(i),i=1,ndat)

c..THEORETICAL y(i)  AS INPUT
            read(9,*)(yth(i),i=1,ndat)

c..INITIAL VALUES AND UNCERTAINITIES OF PARAMETERS AS INPUT
            read(9,*)(p(i),punc(i),i=1,mpar)

c..MATRIX A CONTAINING THE DERIVATIVES  AS INPUT
            read(9,*)((a(i,j),j=1,mpar),i=1,ndat)

C-------------------------------------------------------------
C      ******   DOCUMENTATION OF INPUT FILE AS OUTPUT *******
C-------------------------------------------------------------
       write(nwrite,*)'  NUMBER OF OBSERVATIONS=',ndat
       write(nwrite,*)'  NUMBER OF UNKNOWN PARAMETERS    =',mpar
c       write(nwrite,600)
 600    format(3(/),20x,'    OBSERVED  Y AT Z',/,
   !    23X,'Z',16X,'Y',5x,'Uncertainity of Y'/,10x,59('_'))
c       write(nwrite,610)(i,x(i),y(i),uncy(i),i=1,ndat)
 610  format(9x,i4,4x,d12.5,5x,d12.5,4x,d12.5)

c       write(nwrite,620)
 620  format(3(/),20x,' THEORETICAL Y AT Z',/,
   !23X,'Z',16X,'YTH',/,10x,39('_'))
c       write(nwrite,630)(i,x(i),yth(i),i=1,ndat)
 630  format(9x,i4,4x,d12.5,5x,d12.5)

C-------------------------------------------------------------
C   IF kcode .lt. 0    : OUTPUT TO TERMINAL
C      kcode .gt. 0    : OUTPUT TO OUTPUT FILE
C-------------------------------------------------------------
            kcode=inttwo
            if(ncode.ne.'t')kcode=-kcode
            call umach(kcode,nwrite)
C-------------------------------------------------------------
C   SUBROUTINE wrrrn WRITES THE GIVEN MATRIX OR VECTOR
C   WHEN USED INTZERO IN WRRRN THEN OUTPUT IS FULL MATRIX
C-------------------------------------------------------------
c     call wrrrn
c    !('MATRIX A CONTAINING THE DERIVATIVES',ndat,mpar,a,ndim,intzero)

C-------------------------------------------------------------
C  IF THE UNCERTAINITY FOR ANY OBSERVATION IS TOO BIG, THEN
C  CORRESPONDING DERIVATIVE WITHIN MATRIX A WILL BE SMALLER.THAT
C  IS , THE EFFECT OF THIS OBSERVED DATA ON CALCULATING PARAMETERS
C  WILL BE LESS.
C-------------------------------------------------------------
C     TEST IF ANY OF UNCERTAINITIES OF Y IS EQUAL TO ZERO
C     TO AVOID DIVISION BY ZERO,DIVIDE IT BY EPSILON
C-------------------------------------------------------------
            do 40 i=1,ndat
            if(uncy(i).ne.zero) go to 40
            uncy(i)=epsilon
            write(6,633)i,epsilon
 40          continue
 633  format(3x,'****WARNING*****',/,3X,'UNCERTAINITY FOR THE','/',
   !i6,'/th OBSERVATION WAS EQUAL TO ZERO.IT HAS BEEN CHANGED AS',
   !/,3x,'/',d12.5,'/')
C-------------------------------------------------------------
C     HOLD THE MATRIX A WITHIN MATRIX "AHOLD"
C     TRANSPOSE (DELTA Y)
C     WEIGHTING THE MATRIX A AND DELTA(Y) BY UNCERTAINITY OF Y
C     WEIGHTING THE MATRIX A  BY UNCERTAINITY OF PARAMETERS
C-------------------------------------------------------------
          do 60 i=1,ndat
              tmpr=one/uncy(i)
              ydelta(i)=(y(i)-yth(i))*tmpr
```

```
                do 50 j=1,mpar
                  ahold(i,j)=a(i,j)
                  a(i,j)=a(i,j)*tmpr*punc(j)
 50                continue
 60                continue
c..  WRITE THE WEIGHTED MATRIX A
c     call wrrrn
c     !('WEIGHTED MATRIX A',ndat,mpar,a,ndim,intzero)
        write(nwrite,635)
 635  format(10x,/,'INITIAL MODEL WITH  UNCERTAINITIES',/)
      write(nwrite,636)(i,p(i),punc(i),i=1,mpar)
 636  format(10X,'p0(',i5,')=',d12.5,'     ',d12.5)

C-------------------------------------------------------------
C    CALCULATION OF SCALAR  " R "  FROM INITIAL MODEL
C       Y(calculated) = Matrix (a) * (Initial Parameters)
C       Residuels = Y(observed)- Y(calculated)
C-------------------------------------------------------------
              rscalar=zero
             do 61 i=1,ndat
               rscalar=rscalar+(ydelta(i)**two)
 61           continue
               rscalar=dsqrt(rscalar/(float(ndat)))


C-------------------------------------------------------------
C   ***  SOLUTION WITH IMSL ROUTINES  ***
C-------------------------------------------------------------


C-------------------------------------------------------------------------
C     CALCULATING THE MATRIX U,V,AND SINGULAR VALUES (S) IN ORDER,
C              FROM MAXIMUM TO MINIMUM
C-------------------------------------------------------------------------
C                 ************!!!!!*************
C       LCODE = IJ
C            I=0   DO NOT COMPUTE THE LEFT SINGULAR VECTORS
C            I=1   RETURN THE mpar LEFT SINGULAR VECTORS IN U
C            I=2   RETURN ONLY THE MIN(ndat,mpar) LEFT SINGULAR
C                  VECTORS IN U
C            J=0   DO NOT COMPUTE THE RIGHT SINGULAR VECTORS
C            J=1   RETURN THE RIGHT SINGULAR VECTORS IN V
C-------------------------------------------------------------------------
        call dlsvrr(ndat,mpar,a,ndim,LCODE,tol,irank,
     !                          s,u,ndim,v,ndim)


C-------------------------------------------------------------------------
C   WRITE THE ALL SINGULAR VALUES
C   Note : 1- All Singular values are positive
C          2- s(irank),s(irank+1),..,s(mpar) are defined
C             zero if s(i).le.tol ----> WHERE tol .GE. 0.0
C       DUE TO THE ROUND OFF ERROR , SOME OF SMALL SINGULAR VALUES
C       MAY BE NEGATIVE,TO PREVENT THIS CONDITION, PARAMETER tol
C       "MUST"  BE POSITIVE LOWER BOUND.IF tol IS NEGATIVE THEN
C       THE CONDITION S(I).LE. ABS(TOL) WILL BE CONSIDERED
C-------------------------------------------------------------------------


C-------------------------------------------------------------------------
C   IF THE LAST SINGULAR VALUE IS ZERO , CONDITION NUMBER THEN
C   WILL BE ZERO.   THIS IS THE CASE WHEN ... IRANK.NE.MPAR ....
C-------------------------------------------------------------------------

c..  lamda includes the nonzero singular values

        lamda=min(ndat,mpar)
        numcond=infinit
        if(s(lamda).gt.tol)numcond=s(intone)/s(lamda)
          write(nwrite,699)
        write(nwrite,640)irank,numcond,rscalar
 640  format('Rank =',i4,' /Condition Number=',i5,
   !' /Scalar R(from initial)=',f10.3)
        write(nwrite,645)tol
 645     format(5x,'If the Singular values are  greater than',
   ! d12.5,'  they are counted nonzero, zero othewise.')

c     call wrrrn('ALL SINGULAR VALUES',intone,lamda,s,intone,intzero)
        write(nwrite,*)'All SINGULAR VALUES'
        write(nwrite,996)(i,s(i),i=1,lamda)
 996     format(4x,i4,5x,d20.10)

          write(nwrite,699)
C-------------------------------------------------------------
C    WE ALREADY IGNORE THE ZERO SINGULAR VALUES BY STARTING WITH
C    irank,NUMBER OF NONZERO SINGULAR VALUES AND  CORRESPONDING
C    SINGULAR VECTORS. STARTING IS FROM IGNORING THE MINIMUM
C    THROUGH MAXIMUM. FOLLOWING q IS THE NUMBER OF SING.VAL USED
C-------------------------------------------------------------
          do 99 q=irank,kto,-kstep
C-------------------------------------------------------------
C   CALCULATING THE INVERSE OF THE MATRIX SIGMA
C-------------------------------------------------------------
               do 100 i=1,q
                 do 90 j=1,q
                   ve(i,j)=zero
                   if(i.eq.j)ve(i,j)=one/s(i)
 90                continue
 100                continue
C-------------------------------------------------------------
C   WRITE SINGULAR VALUES USED
C-------------------------------------------------------------
          numcond=s(intone)/s(q)
```

```
          write(nwrite,650)numcond,lamda,q
650  format(1X,'Condition Number',i8,', Max q=',i8,
     !',--->Solution when q ='i8)
c      call wrrrn('SINGULAR VALUES USED',intone,q,s,intone,intzero)

C-----------------------------------------------------------------
C    CALCULATING THE V*INVERS(SIGMA)
C-----------------------------------------------------------------
       call dmrrrr(mpar,q,v,ndim,q,q,ve,ndim,
     !                        mpar,q,vve,ndim)
C-----------------------------------------------------------------
C   CALULATING THE MATRIX  H =  V*INV(SIGMA)*TRANSPOSE(U)
C-----------------------------------------------------------------
       call dmxytf(mpar,q,vve,ndim,ndat,q,u,ndim,
     !                        mpar,ndat,vveu,ndim)

C-----------------------------------------------------------------
C    MULTIPLICATION MATRIX H BY VECTOR DELTA Y
C         ICODE =1 MEANS THE PRODUCT  Y-= A*X IS COMPUTED
C         ICODE =2 MEANS THE PRODUCT  Y-= transpose(A)*X IS COMPUTED
C-----------------------------------------------------------------
       call dmurrv(mpar,ndat,vveu,ndim,ndat,ydelta,ICODE,mpar,pcalc)
                  do 130 k=1,mpar
                    pcalc(k)=pcalc(k)*punc(k)
                    pcalc(k)=p(k)+pcalc(k)
130                  continue

C-----------------------------------------------------------------
C      SCALAR R, WHEN q=IRANK,IRANK-1,IRANK-2, .... ,1
C       Y(calculated) = Matrix (a) * (Calculated Parameters)
C       Residuels = Y(observed)- Y(calculated)
C-----------------------------------------------------------------
     call dmurrv(ndat,mpar,ahold,ndim,mpar,pcalc,ICODE,ndat,ycalc)
           rqscalar=zero
           do 125 i=1,ndat
             residual=y(i)-ycalc(i)
             reciprocal=one/uncy(i)
             rqscalar=rqscalar+(residual*reciprocal)**two
125           continue
             rqscalar=dsqrt(rqscalar/(float(ndat)))

C-----------------------------------------------------------------
C        CALCULATION OF THE VARIANCES OF THE PARAMETERS
C-----------------------------------------------------------------
                do 150 i=1,mpar
                  uncp(i)=zero
                  do 140 j=1,q
                  uncp(i)=uncp(i)+(v(i,j)/s(j))**two
140                 continue
                  uncp(i)=dsqrt(uncp(i))*punc(i)
150               continue
C-----------------------------------------------------------------
C   CALCULATION OF MATRIX R
C-----------------------------------------------------------------
       call dmxytf(mpar,q,v,ndim,mpar,q,v,ndim,
     !                        mpar,mpar,rm,ndim)
C-----------------------------------------------------------------
C   CALCULATION OF MATRIX S
C-----------------------------------------------------------------
       call dmxytf(ndat,q,u,ndim,ndat,q,u,ndim,
     !                        ndat,ndat,sm,ndim)


C-----------------------------------------------------------------
C   QUANTITY rk
C-----------------------------------------------------------------
                do 180 k=1,mpar
                  sumi=zero
                do 170 i=1,mpar
                  sumj=zero
                do 160 j=1,q
                  sumj=sumj+(v(k,j)*v(i,j))
160         continue
                  delta=zero
                  if(k.eq.i)delta=one
                  sumi=sumi+(sumj-delta)**two

170         continue
                  rk(k)=sumi
180         continue


C-----------------------------------------------------------
C  WRITE THE CALCULATED  MATRIXES
C-----------------------------------------------------------------
c      call wrrrn('MATRIX V',mpar,q,v,ndim,intzero)
c      call wrrrn('MATRIX U',ndat,q,u,ndim,intzero)
c      call wrrrn('MATRIX H',mpar,ndat,vveu,ndim,intzero)
c      call wrrrn('MATRIX S',ndat,ndat,sm,ndim,intzero)
c      call wrrrn('MATRIX R',mpar,mpar,rm,ndim,intzero)
C-----------------------------------------------------------



     write(nwrite,655)rqscalar
655   format(3(/),10x,'Scalar R =',f10.3)
     write(nwrite,660)
660  format(10x,
    !'CALCULATED PARAMETERS,     UNCERTAINITIES,   QUANTITY r',
    !/,10x,55('_'),)
```

```
      write(nwrite,670)(i,pcalc(i),uncp(i),rk(i),i=1,mpar)
C 670  format(10X,'par(',i5,')=',f12.0,'     ',f10.0,'   ',f10.3)
      write(nwrite,699)
 99       continue
 699  format(5x,/,74('='),//)
C-------------------------------------------------------------------
C          ****** CLOSE OPENED FILES *****
C-------------------------------------------------------------------
      if(ncode.NE.'t')close(unit=nwrite)
                      close(unit=9)
                      go to 998
```

```
999               continue
      write(6,*)' >>>>> ERROR <<<<< '
      write(6,*)' >>>>>THE NUMBER OF PARAMETERS AND/OR'
      write(6,*)' >>>>>OBSERVATIONS ARE GREATER THAN /',ndim,'/'
      write(6,*)' >>>>>CNANGE THE PARAMETER 'ndim=',mpar
      write(6,*)' >>>>>AT THE 'parameter' STATEMENT IN THIS '
     write(6,*)' >>>>>PROGRAM AND RECOMPILE'
998             stop'                          >>>>>    BYE  '
               end
```